

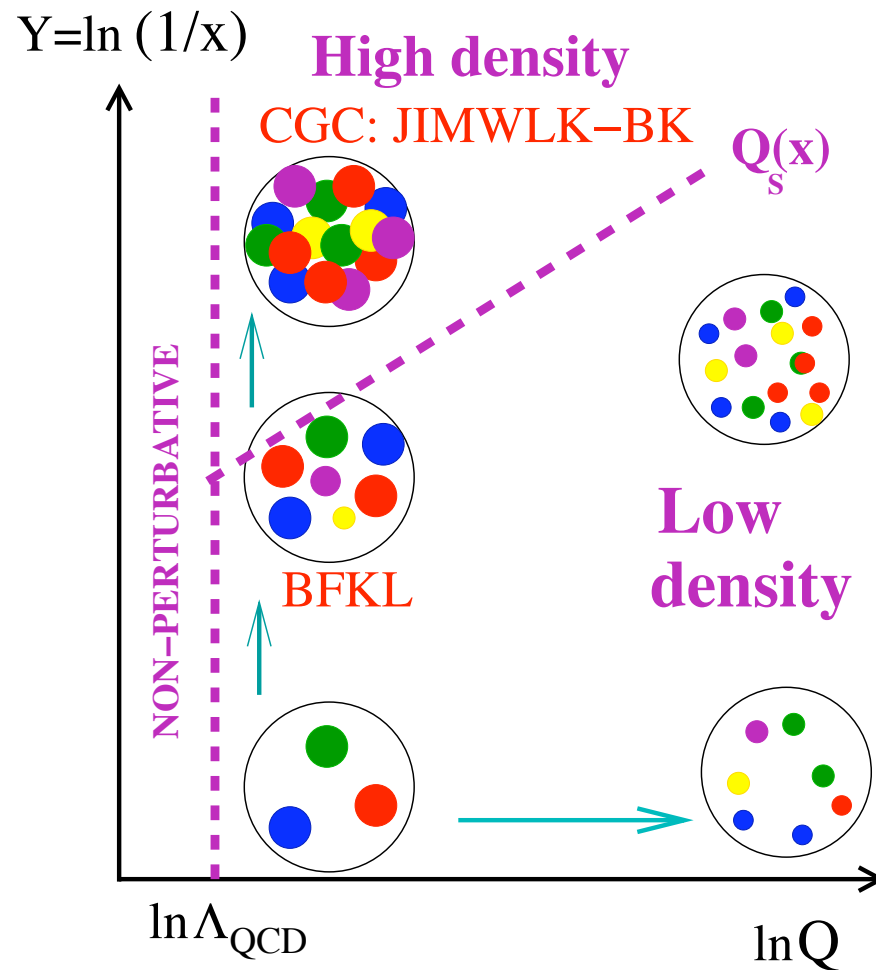
# *Dipole models in inclusive observables at the LHeC*

Javier L. Albacete  
IPhT-CEA-Saclay

**2nd CERN-ECFA-NuPECC Workshop on the LHeC  
Divonne Les Bains, 1-3 September 09**



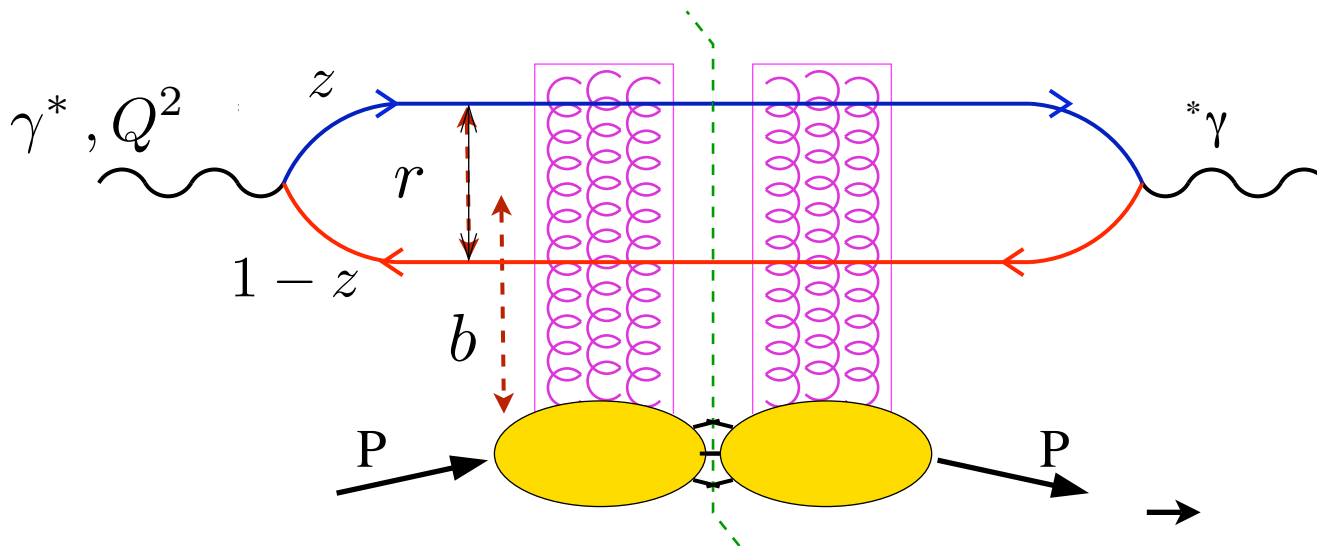
⇒ **Saturation:** At small Bjorken- $x$  the hadron wave function gets dense and non-linear processes become a relevant dynamical ingredient



⇒ One of the potential goals (duties) of the LHeC is to turn the sketch above into something quantitative.

# Dipole model of DIS

- ⇒ It stems from kt-factorization theorem in the limit  $x \rightarrow 0$  (Nikolaev-Zakharov-Mueller)
- ⇒ DIS x sections: Convolution of photon wavefunction with dipole cross section



$$\sigma_{T,L}^{\gamma^* P}(x, Q^2) = \int_0^1 dz \int d^2 \mathbf{r} \left| \Psi_{T,L}^{\gamma^* \rightarrow q\bar{q}}(z, Q, r) \right|^2 \sigma^{dip}(x, r)$$

**Photon wavefunction**  
Calculable within QED

**Dipole cross section.**  
Strong interactions and  
x-dependence are here

$$\sigma^{dip}(x, r) = 2 \int d^2 b \mathcal{N}(x, b, r)$$

# Saturation in the dipole model

$$\mathcal{N}(r, b, x) = 1 - \exp(-\Omega(r, b, x, \dots))$$

**Unitarity: Black disc limit**

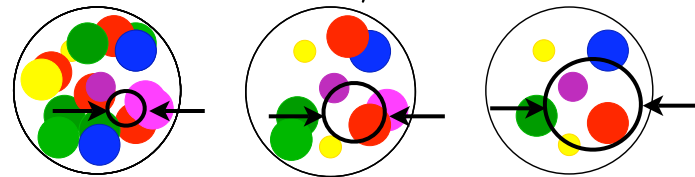
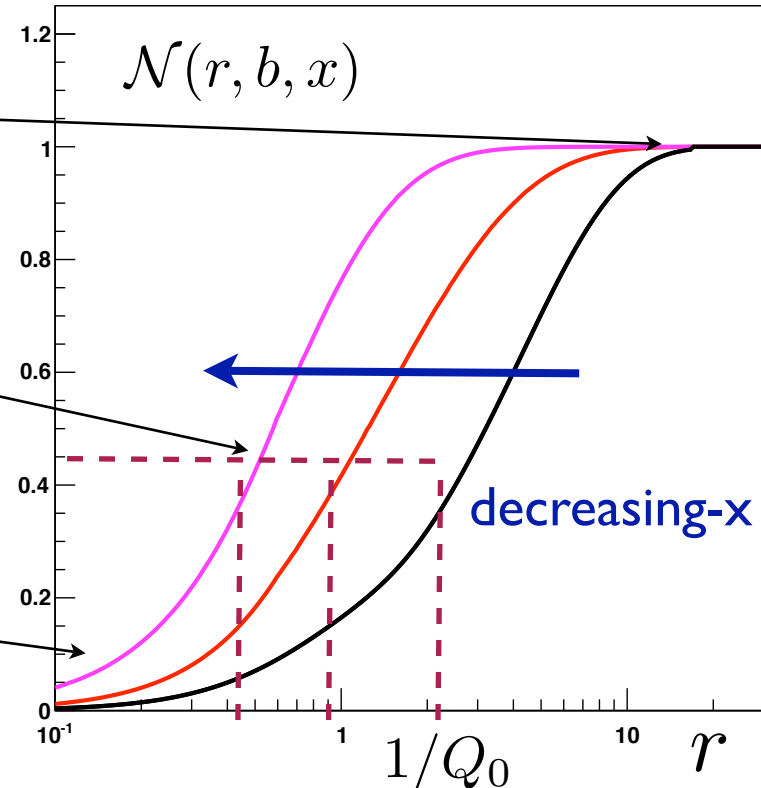
$$\mathcal{N}(r, b, x) \leq 1 \quad \sigma^{\gamma^*p} \leq 2\pi R_p^2(s)$$

**Saturation**

$$\mathcal{N}(r = 1/Q_s(x, b), b, x) \sim 0.5$$

**Dilute, perturbative domain**

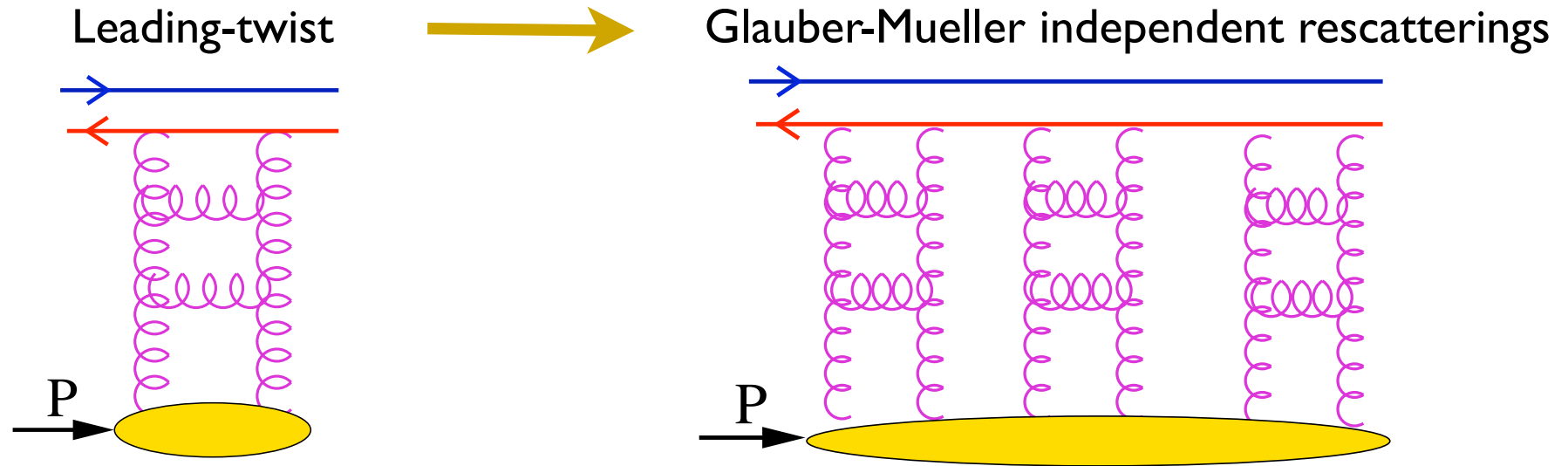
$$\mathcal{N}(r, x) \sim r^2$$



# (My) classification of dipole models in the market

- ⇒ According to the physical mechanism driving saturation, i.e.  $(x, Q^2, r)$ -dynamics:
  - DGLAP.
  - BK or BFKL+saturation
  - Phenomenological models: Regge Theory; non-perturbative input.
- ⇒ According to the  $t$ -dependence (impact parameter dependence)
- ⇒ According to phenomenological details: quark masses, inclusion of charm or beauty contributions, focus on specific kinematic region ...

⇒ **DGLAP-based models:** Saturation results from eikonalization of two-gluon exchange: **BGBK** (Bartels-Golec-Biernat-Kowalski); **IPSat** (Kowalski-Teaney):



$$\frac{d\sigma^{dip}}{d^2b} \sim \frac{\pi^2}{2 N_c} r^2 xg(x, Q^2)T_p(b)$$

$$\frac{d\sigma^{dip}}{d^2b} = 1 - \exp \left[ -\frac{\pi^2}{2 N_c} r^2 xg(x, Q^2)T_p(b) \right]$$

Leading  $\ln Q^2$  terms in each cascade resummed through DGLAP

All the Bjorken- $x$  dependence is encoded in that of the gluon distribution.

**BGBK:** Trivial impact parameter dependence:  $T_p(b) \sim Q_0^2 \theta(b_p - b)$

**IPSat:** Gaussian profile

$$T_p(b) \sim \exp(-b^2/2B)/(2\pi B)$$

⇒ **DGLAP-based models**: Saturation results from eikonalization of two-gluon exchange: **BGBK** (Bartels-Golec-Biernat-Kowalski); **IPSat** (Kowalski-Teaney):

$$\frac{d\sigma^{dip}}{d^2b} = 1 - \exp \left[ -\frac{\pi^2}{2 N_c} r^2 xg(x, \mu^2) T_p(b) \right]$$

$$\mu^2 = \frac{C}{r^2} + \mu_0^2$$

- The **gluon distribution is fitted to data** using the initial parametrization:

$$xg(x, Q_0^2 = 1 \text{ GeV}^2) = A_g x^{-\lambda_g} (1 - x)^{5.6}$$

- The gluon distribution is poorly constrained by data. Good fits for

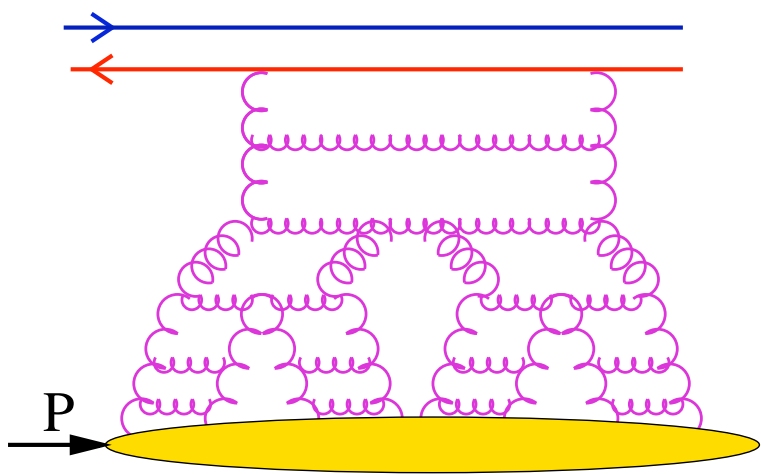
$$-0.41 < \lambda_{glue} < 0.3$$



- Large uncertainties when extrapolating towards small-x. However, very good description of HERA exclusive and diffractive data (IPSat)

## ⇒ Non-Linear Balitsky-Kovchegov equation or Color-Glass-Condensate:

$$\frac{\partial \mathcal{N}(r, x)}{\partial \ln(x_0/x)} = \int d^2 r_1 K(r, r_1, r_2) [\mathcal{N}(r_1, x) + \mathcal{N}(r_2, x) - \mathcal{N}(r, x) - \mathcal{N}(r_1, x)\mathcal{N}(r_2, x)]$$

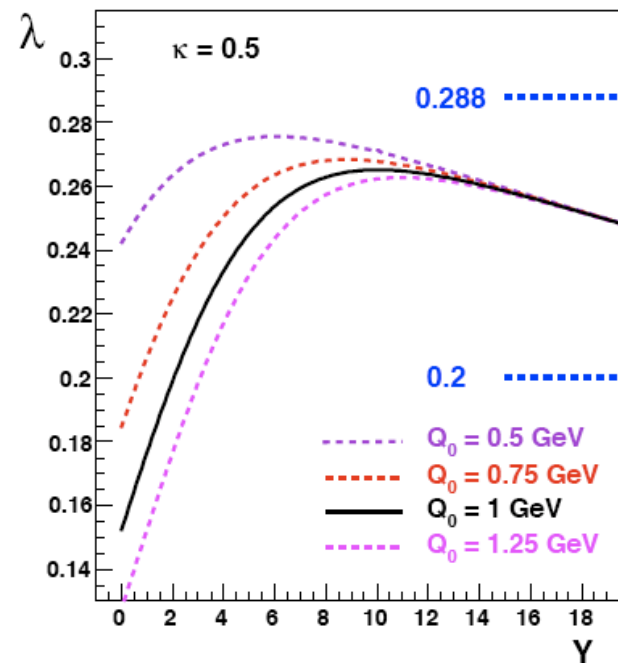
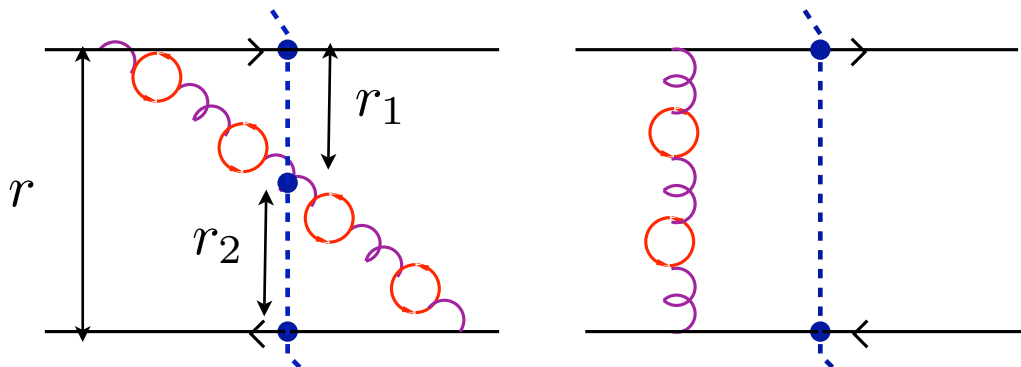


⇒ Resums “fan” diagrams and leading  $\alpha_s \ln 1/x$  terms

⇒ The LL in  $\alpha_s \ln 1/x$  eqn fails to describe data. **Running coupling effects** to the evolution kernel render BK equation compatible with data.

$$Q_s^2(x) \sim x^{-\lambda} \Rightarrow \begin{cases} \lambda^{LL} \sim 4.8 \alpha_s \\ \lambda^{RUN} \sim 0.15 \div 0.3 \end{cases}$$

Evolution kernel: Soft gluon emission plus running coupling corrections (pQCD)





## ⇒ Non-Linear Balitsky-Kovchegov equation or Color-Glass-Condensate:

$$\frac{\partial \mathcal{N}(r, x)}{\partial \ln(x_0/x)} = \int d^2 r_1 K(r, r_1, r_2) [\mathcal{N}(r_1, x) + \mathcal{N}(r_2, x) - \mathcal{N}(r, x) - \mathcal{N}(r_1, x)\mathcal{N}(r_2, x)]$$

A) Calculations based on numerical solutions of BK eqn with running coupling  
JLA-Armesto-Milhano-Salgado (AAMS), Kuokkanen-Rummukainen-Weigert (KRW).

- Trivial impact parameter dependence. Overall normalization fitted to data
- Input: Initial conditions for the evolution,  $\mathcal{N}(r, x_0)$  (GBW, G-M, scaling)
- KRW: Energy conservation (i.e., large-x) effects implemented through

$$K \longrightarrow \left( 1 - \frac{\partial}{\partial \ln(x_0/x)} \right) K$$

B) Models based on analytical solutions of BFKL+ absorptive barrier  
Iancu-Itakura-Munier-Soyez (CGC), Kowalski-Motyka-Watt (b-CGC)

- Evolution speed  $\lambda$  fitted to data
- b-CGC: Impact parameter dependence.

Bad  $\chi/\text{d.o.f} \sim 1.6$ . Lowest evolution speed of all models:  $\lambda \sim 0.16$

C) Hybrid BK (large-r)+DGLAP (small-r) + gaussian impact parameter approach  
Gotsman-Levin-Lublinsky-Maor

## ⇒ Phenomenological models

A) Golec-Biernat-Wusthoff

$$\left\{ \begin{array}{l} \mathcal{N}^{GBW}(x, r) = \theta(R_p - b) \left( 1 - \exp \left[ -\frac{r^2 Q_s^2(x)}{4} \right] \right) \\ Q_s^2(x) = Q_0^2 \left( \frac{x_0}{x} \right)^\lambda \end{array} \right.$$

B) Models based on Regge Theory.  
Forshaw-Shaw (FS04).

FS04:  $\sigma^{dip}(r, x) = \left\{ \begin{array}{l} A^{soft} x^{-\lambda_{soft}}, \quad \text{for } r > r_1 \quad (\lambda_{soft} \sim 0.66) \\ A^{hard} r^2 x^{-\lambda_{hard}}, \quad \text{for } r < r_0 \quad (\lambda_{hard} 0.34) \end{array} \right.$

Saturation: The boundary  $r_0$  is dynamical

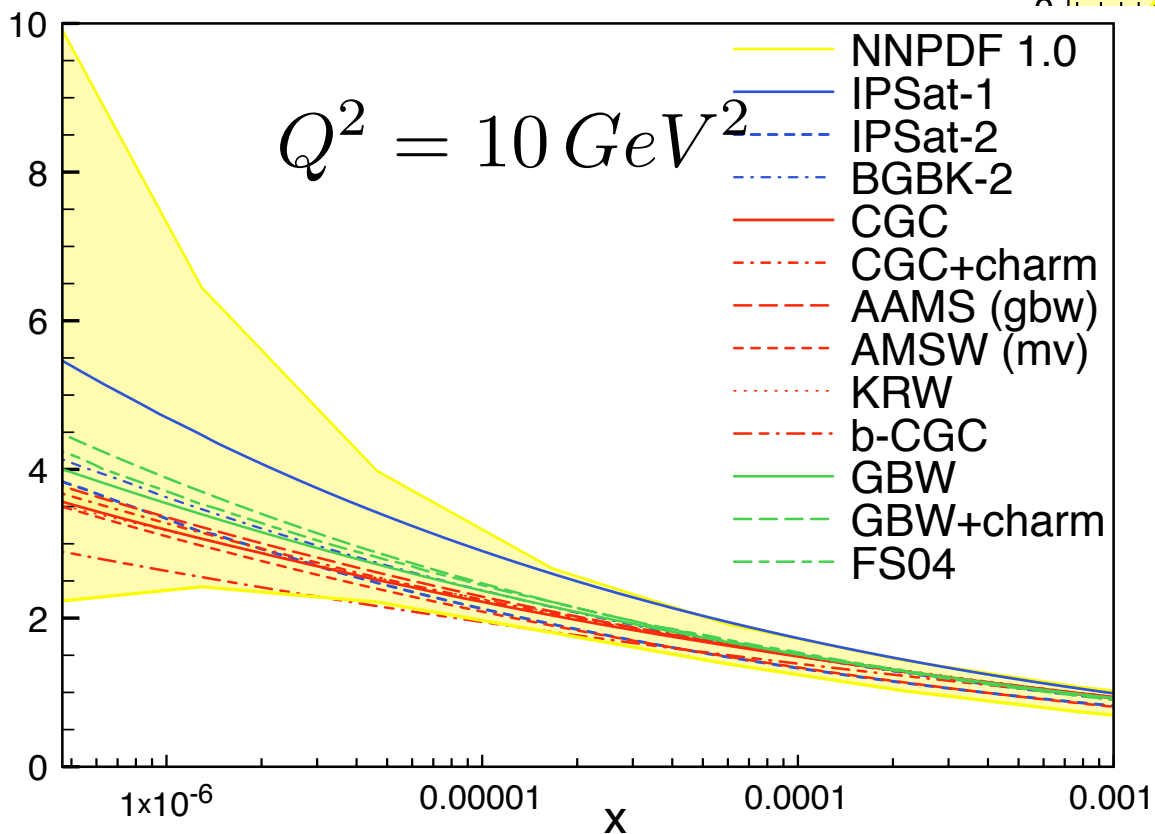
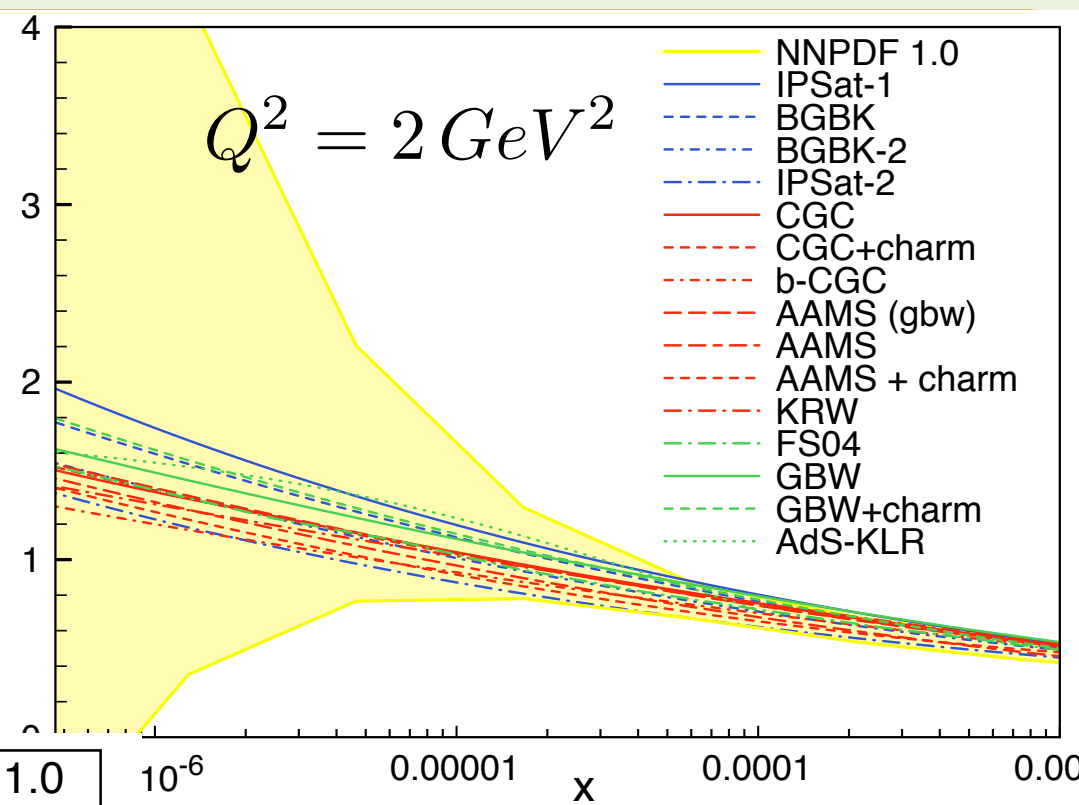
C) Strong coupling dipole from AdS/CFT. Kovchegov-Lu-Rezaeian (appeared this week)

- Valid in the photo production region:  $Q^2 < 2 \text{ GeV}^2$
- Main feature: “Saturation of saturation”:  $Q_s^2(x) \rightarrow \text{constant}, \quad \text{for } x \rightarrow 0$

D) Models tuned to fit also RHIC data.

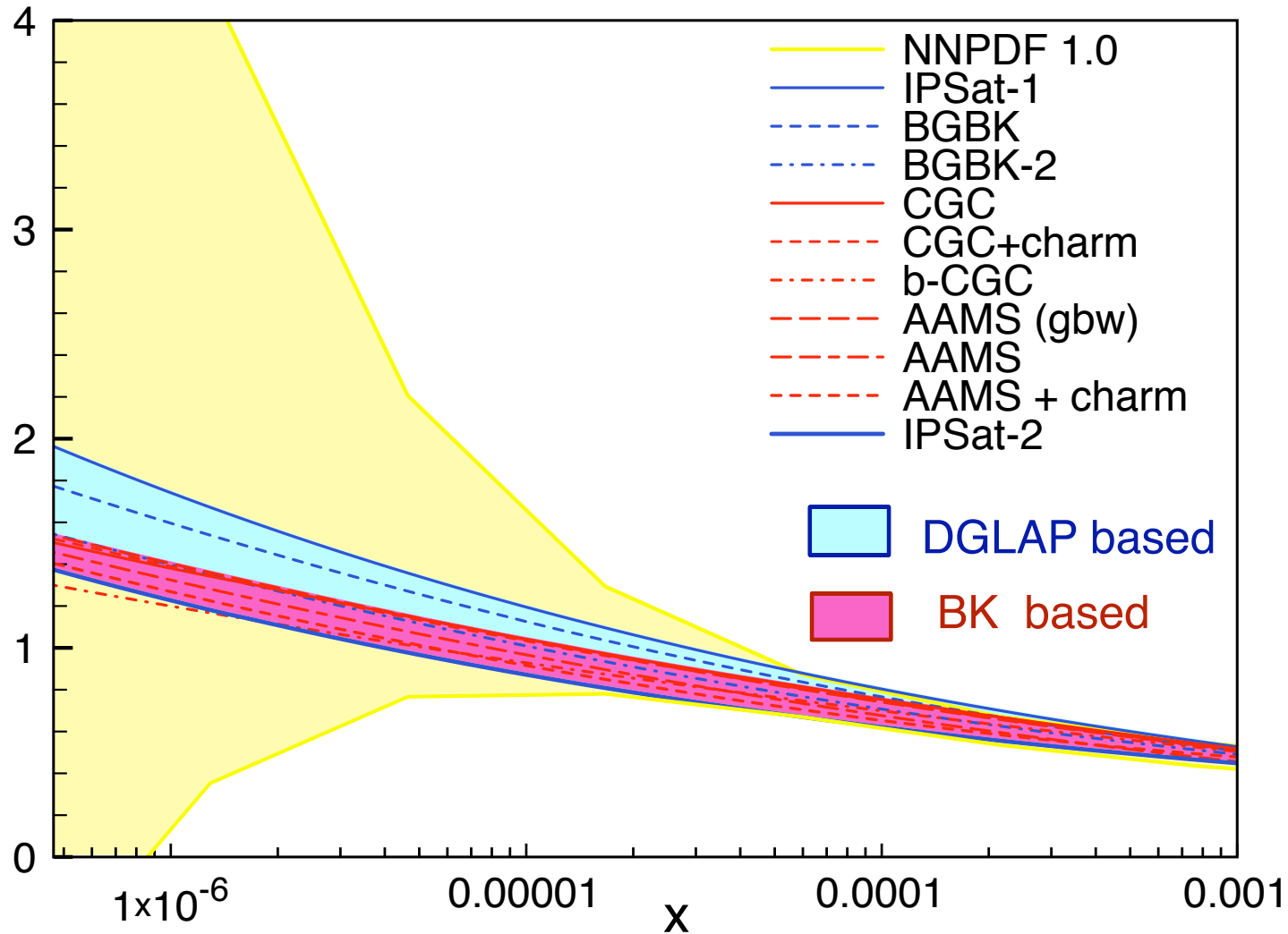
E) Others (my apologies).

# Extrapolation for F2 in the LHeC kinematic regime:



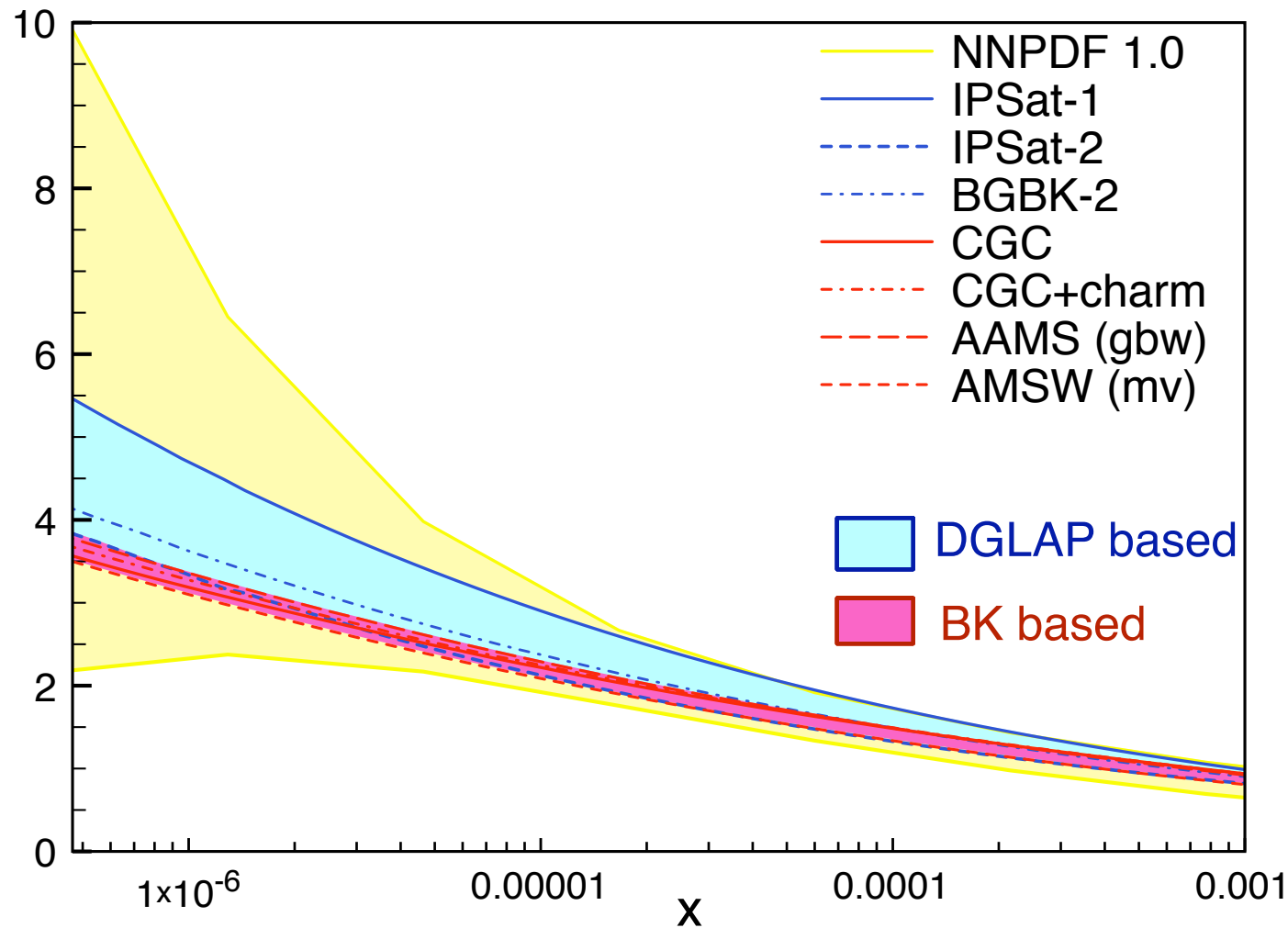
# Extrapolation of the models for $F_2$ : Only BK vs DGLAP

$$F_2(x, Q^2) \quad Q^2 = 2 \text{ GeV}^2$$

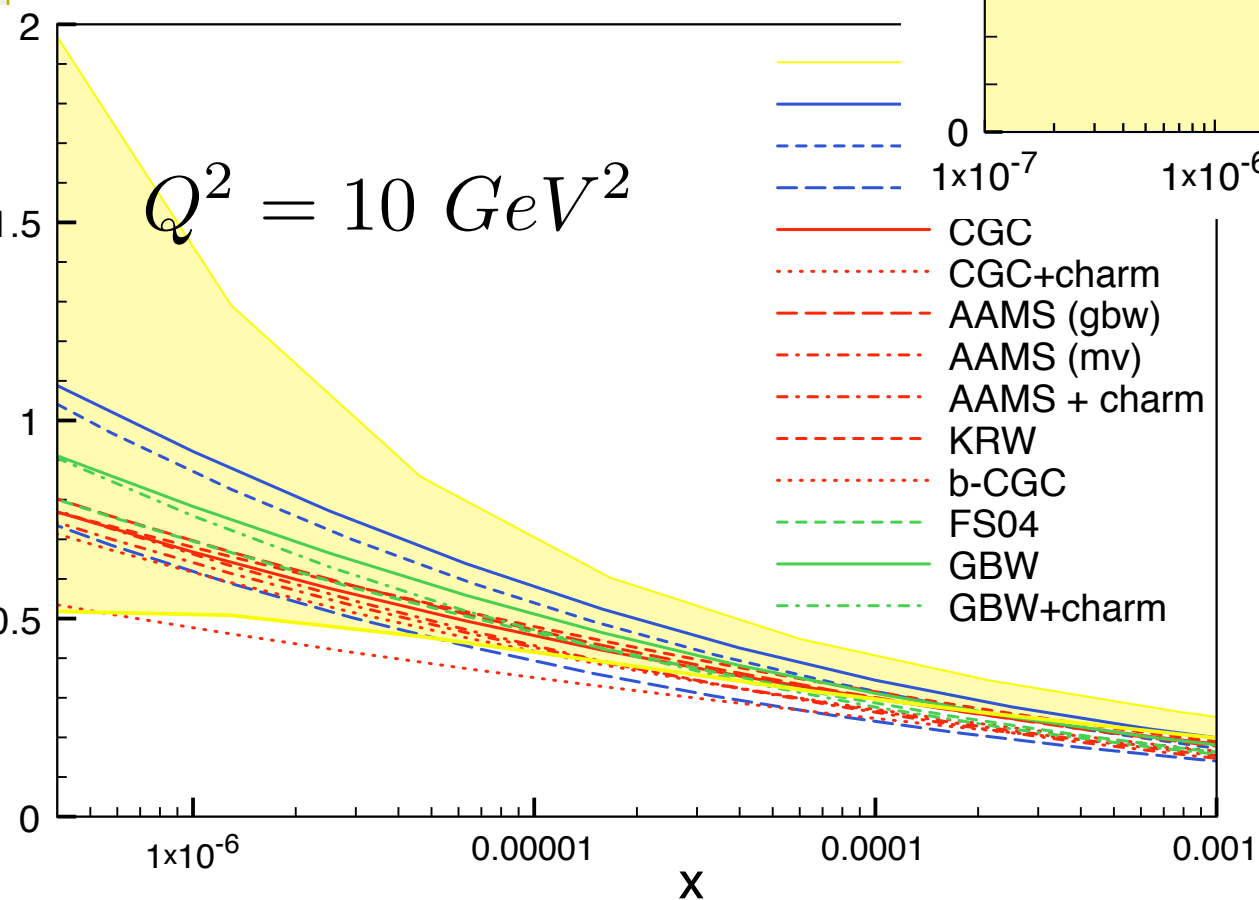
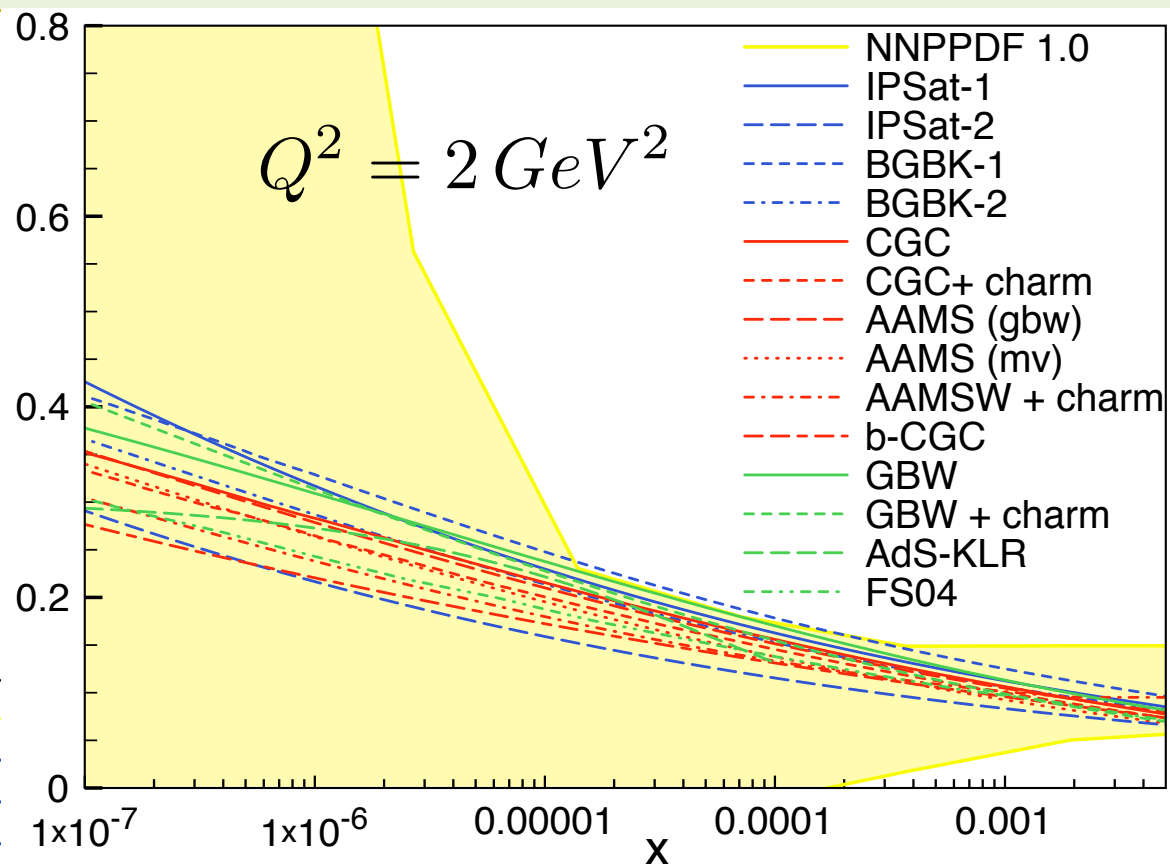


**Extrapolation of the models for F2 : Only BK vs DGLAP (b-CGC removed on account of dab  $\chi^2/\text{dof} \sim 1.6$ )**

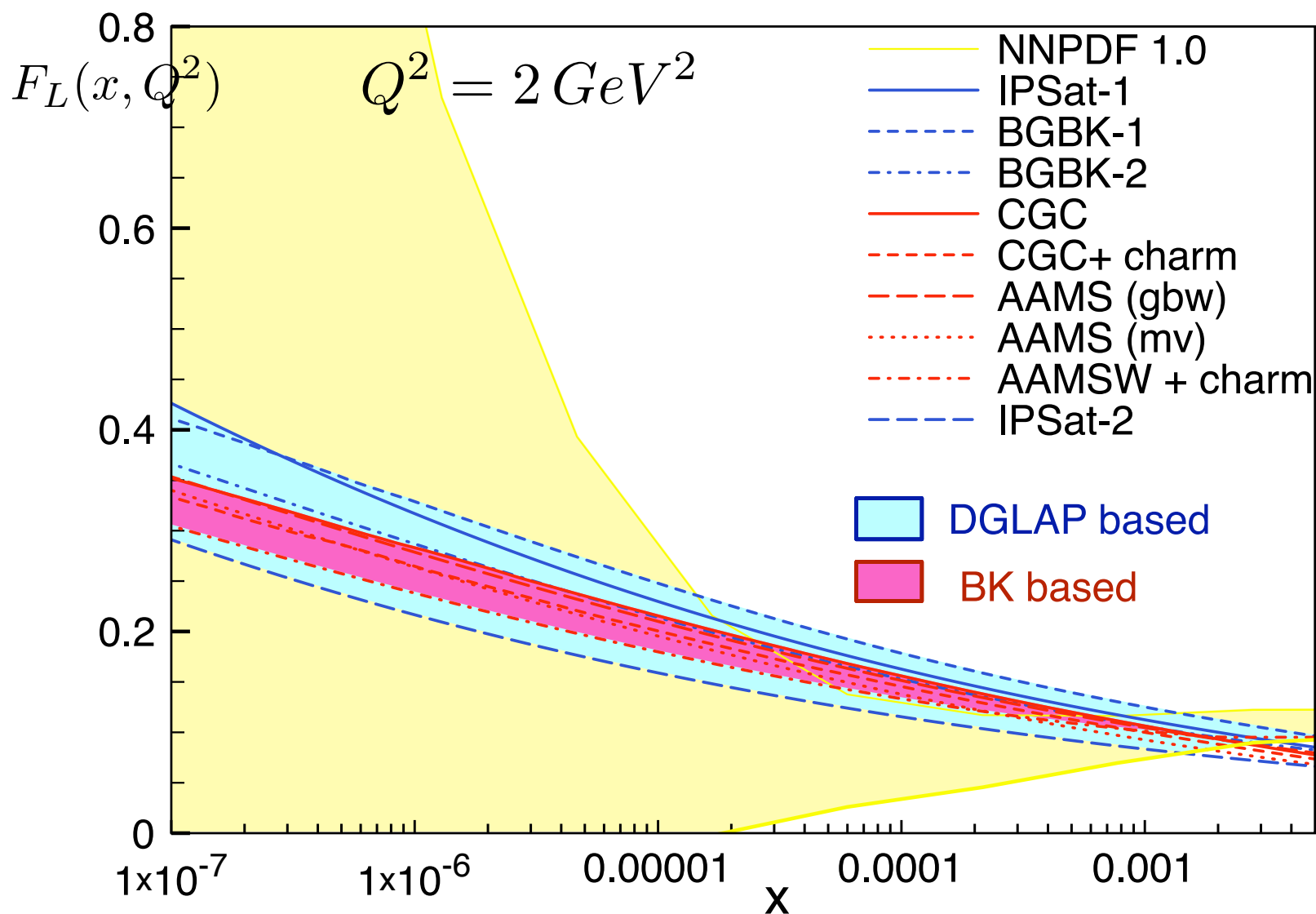
$$F_2(x, Q^2) \quad Q^2 = 10 \text{ GeV}^2$$



# Extrapolation of the models for FL:

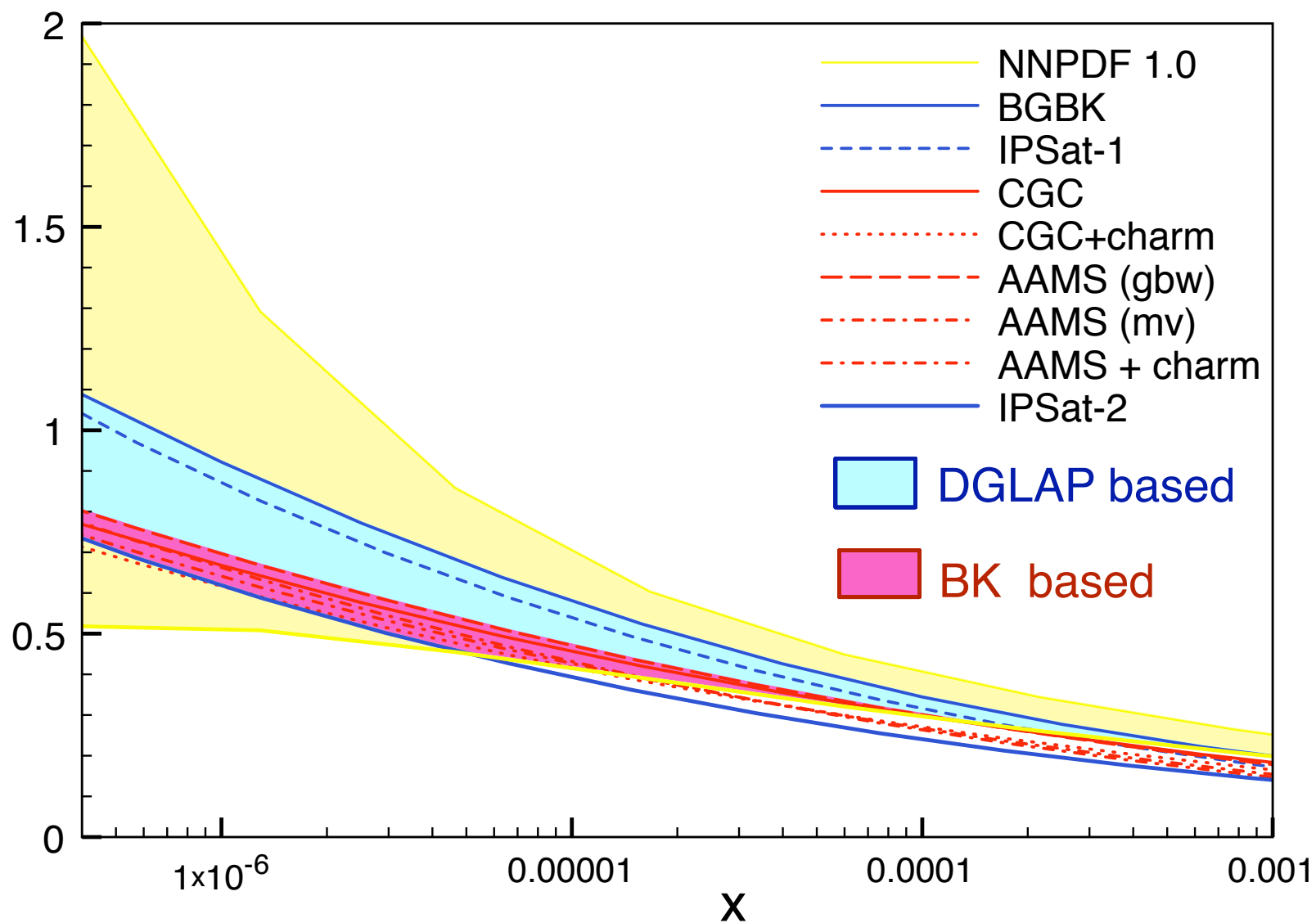


**Extrapolation of the models for FL: Only BK vs DGLAP (b-CGC removed on account of dab  $\chi^2/\text{dof} \sim 1.6$ )**



**Extrapolation of the models for FL: Only BK vs DGLAP (b-CGC removed on account of dab  $\chi^2/\text{dof} \sim 1.6$ )**

$$F_L(x, Q^2) \quad Q^2 = 10 \text{ GeV}^2$$



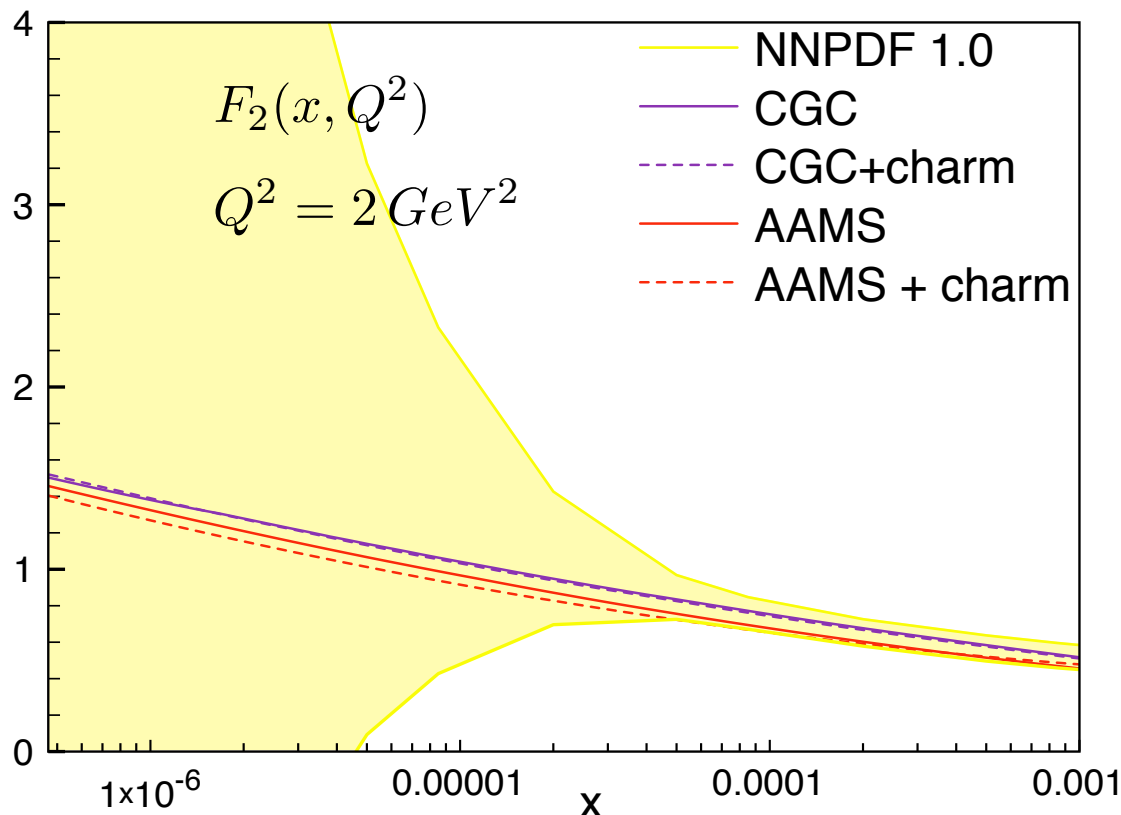


# Quark masses

$$\sigma_{T,L}^{\gamma^* P}(x, Q^2) = \sum_{flavors} \int_0^1 dz \int d^2\mathbf{r} \left| \Psi_{T,L}^{\gamma^* \rightarrow q\bar{q}}(z, Q, r, m_f) \right|^2 \sigma^{dip}(\tilde{x}, r)$$

$$\tilde{x} = x \left( 1 + \frac{4m_f^2}{Q^2} \right)$$

- **Light flavors (u,d,s):**  $0 < m_{u,d,s} < 140 \text{ MeV}$ . Fits in the photoproduction region demand a large (pion) mass.
- **Charm (& beauty):** Needed in order to reproduce measured  $F_2^{charm}$
- Extrapolations are stable after switching on the charm. Values of the saturation scale change.



$$Q_s^2(x) = \left( \frac{x_0}{x} \right)^\lambda \text{ GeV}^2$$

$x_0 / 10^{-4}$	charm	no charm
GBW	0.41	3
CGC	0.1	0.27

# Impact parameter dependence

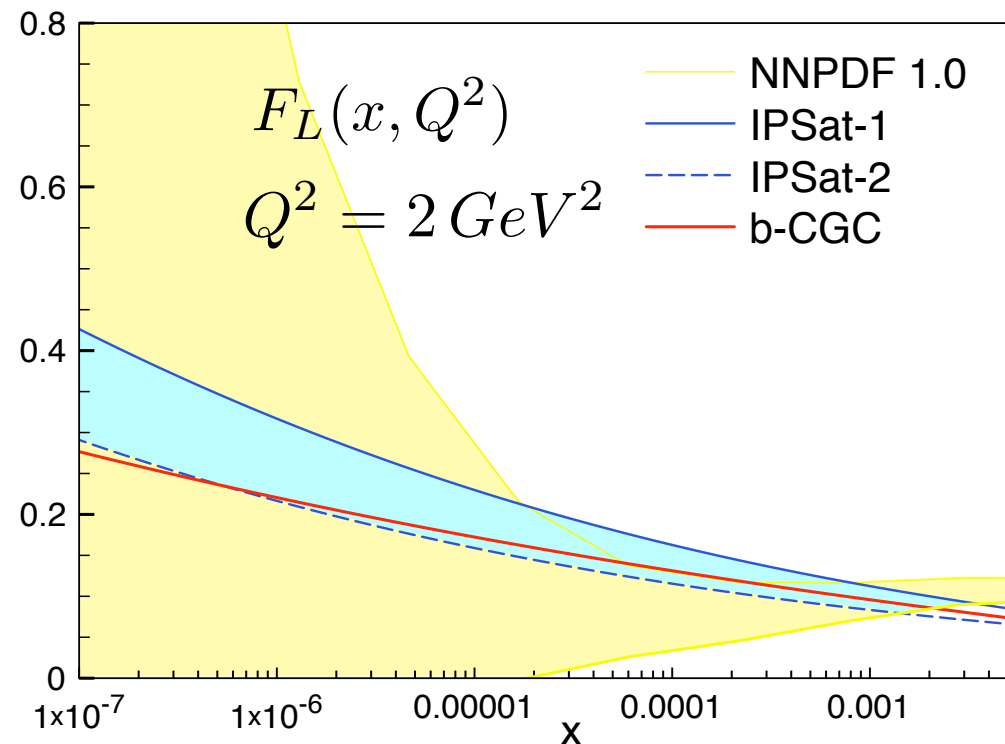
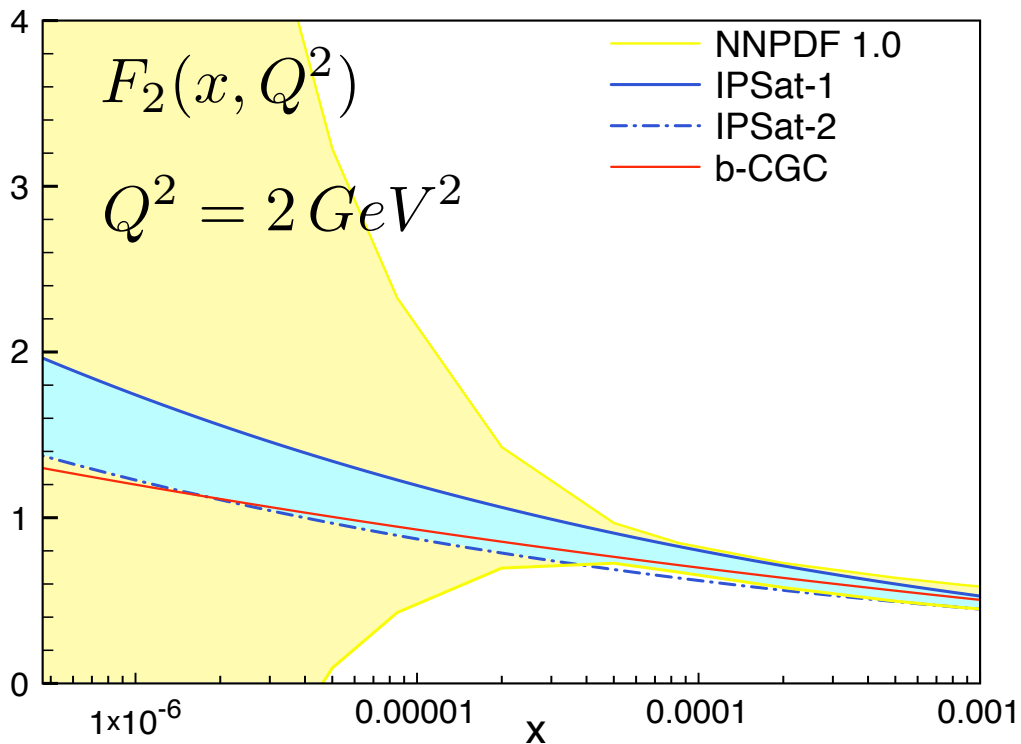
- Only two of the models shown include impact parameter dependence (crucial physical ingredient for exclusive measurements, diffraction ...)

- IPSat: Good description of exclusive observables (VM, DVCS, Diffraction) at HERA

Poor extrapolation to small-x

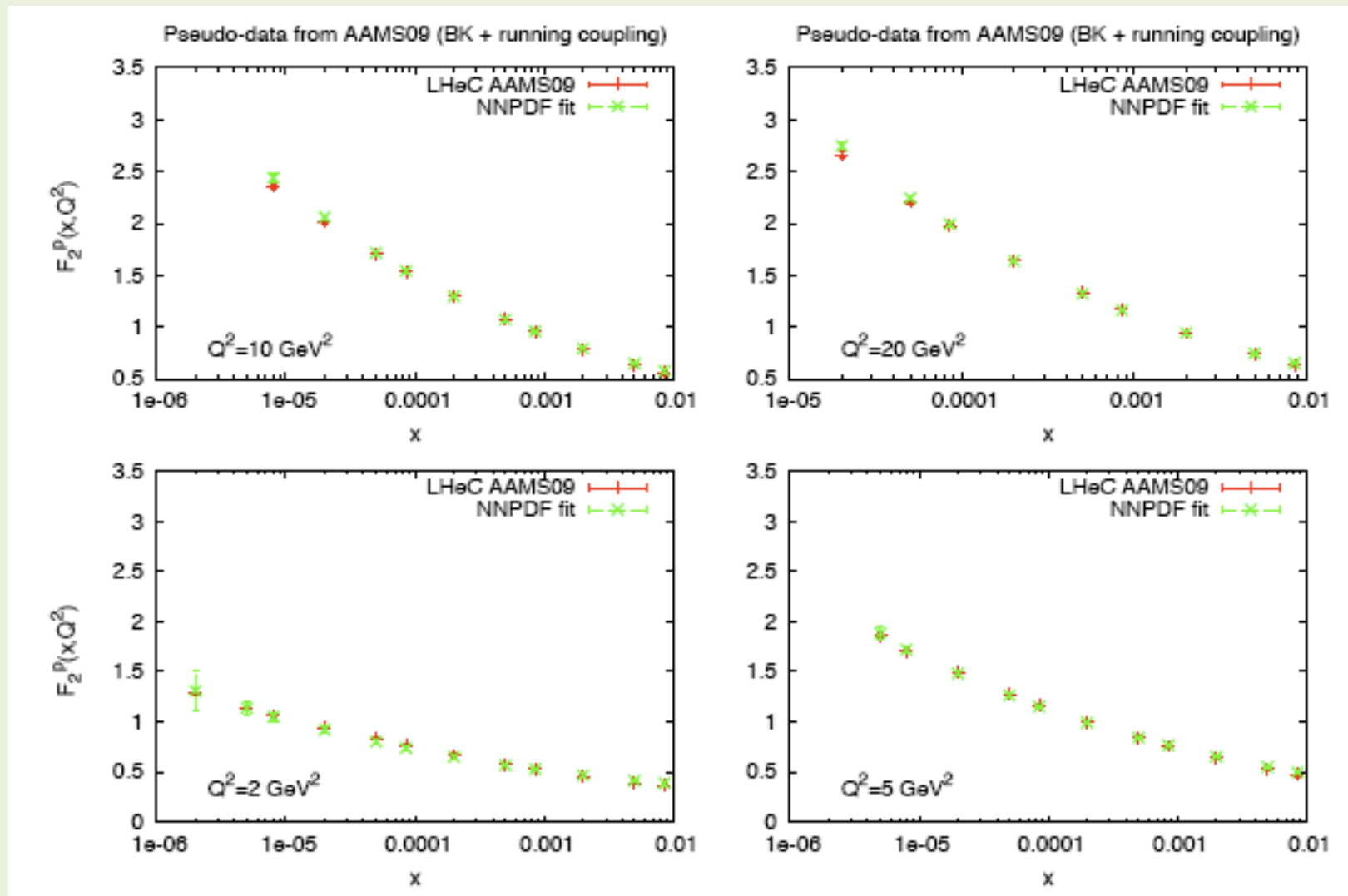
- b-CGC: Not so good description of HERA data.  $\chi/d.o.f \sim 1.6$ . Lowest evolution

speed of all models:  $\lambda \sim 0.16$

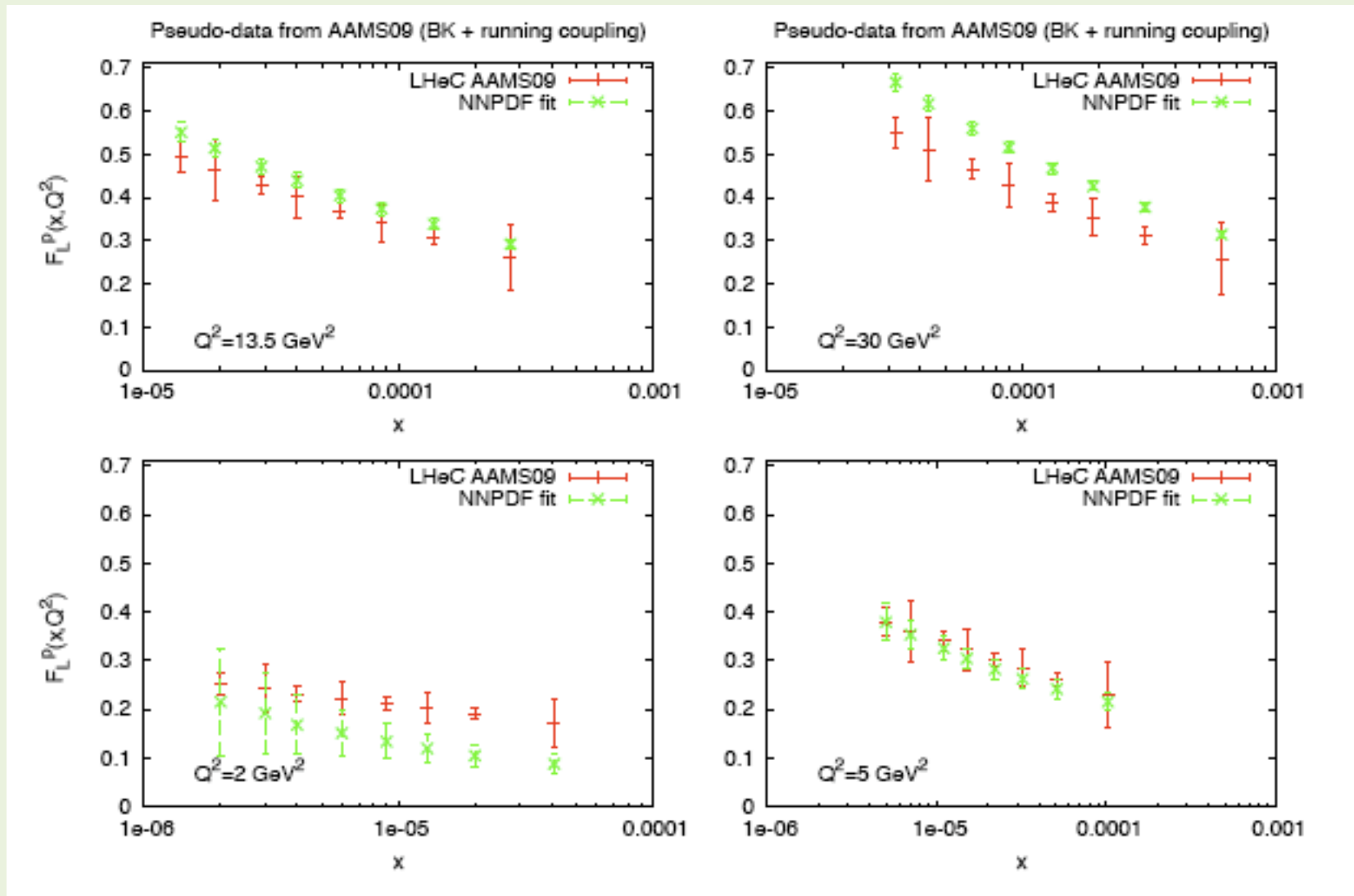


⇒ BK vs DGLAP at small-x (Figs by Juan Rojo):

DGLAP (NNPDF fit) can fit pseudo-data for  $F_2$  at small-x generated by BK with running coupling:



## ⇒ BK vs DGLAP at small-x (Figsto Juan Rojo):



The divergence between linear DGLAP analyses and non-linear small-x dynamics is visible in FL already for  $x \sim 10^{-4}$

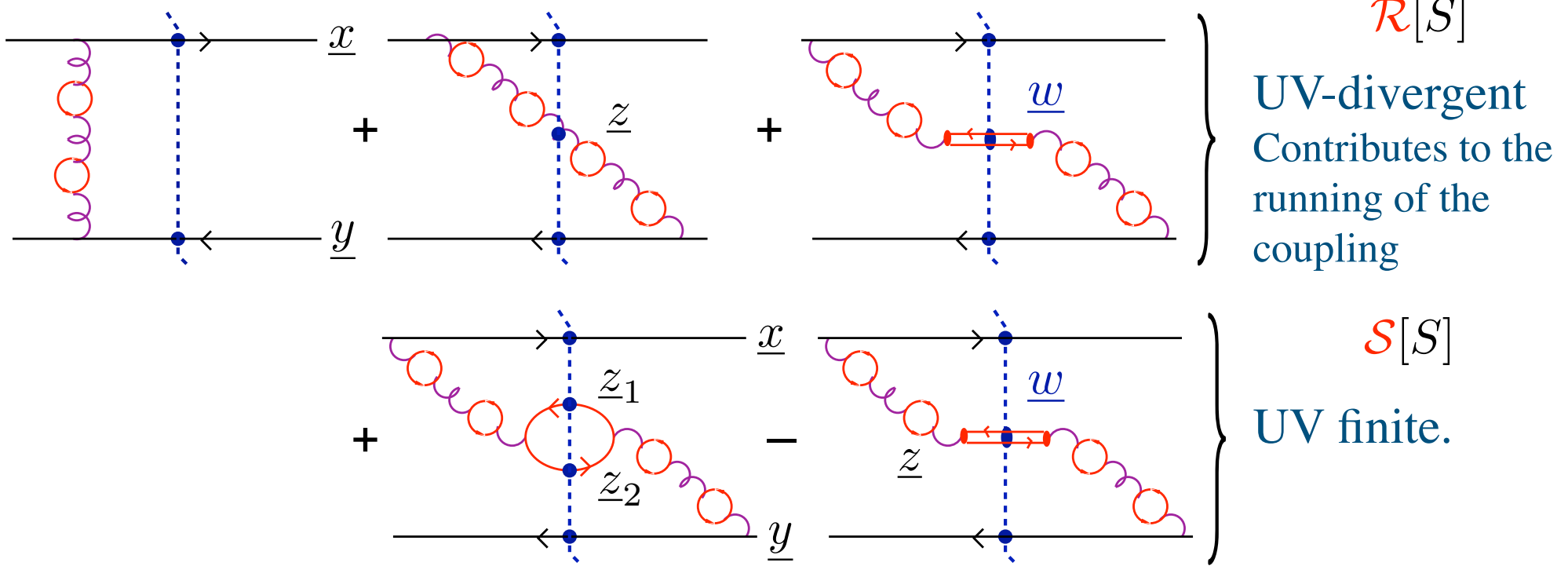
## Conclusions/Outlook

- Little spread in LHeC extrapolations for FL and F2 from different dipole models
- The BK equation (including all recently calculated corrections) provides a solid, pQCD based tool for evolution towards small- $x$
- A more satisfactory implementation of both charm effects and impact parameter dependence is crucial to describe exclusive observable and, possibly nuclear data.

- Parametrizations of the proton-dipole amplitude available at  
<http://www-fp.usc.es/phenom/software.html>



$$\frac{\partial S}{\partial Y} = \mathcal{R}[S] - \mathcal{S}[S]$$



⇒ **Running term:**  $\mathcal{R}[S] = \int d^2 z \tilde{K}(\underline{x}, \underline{z}, \underline{y}) [S(\underline{x}, \underline{z})S(\underline{z}, \underline{y}) - S(\underline{x}, \underline{y})]$

⇒ **Subtraction term:**  $\mathcal{S}[S] = \int d^2 z_1 d^2 z_2 K_{sub}(\underline{x}, \underline{y}, \underline{z}_1, \underline{z}_2) [S(\underline{x}, \underline{w})S(\underline{w}, \underline{y}) - S(\underline{x}, \underline{z}_1)S(\underline{z}_2, \underline{y})]$

Two different separation schemes: Balitsky's (BAL) and Kovchegov-Weigert's (KW)

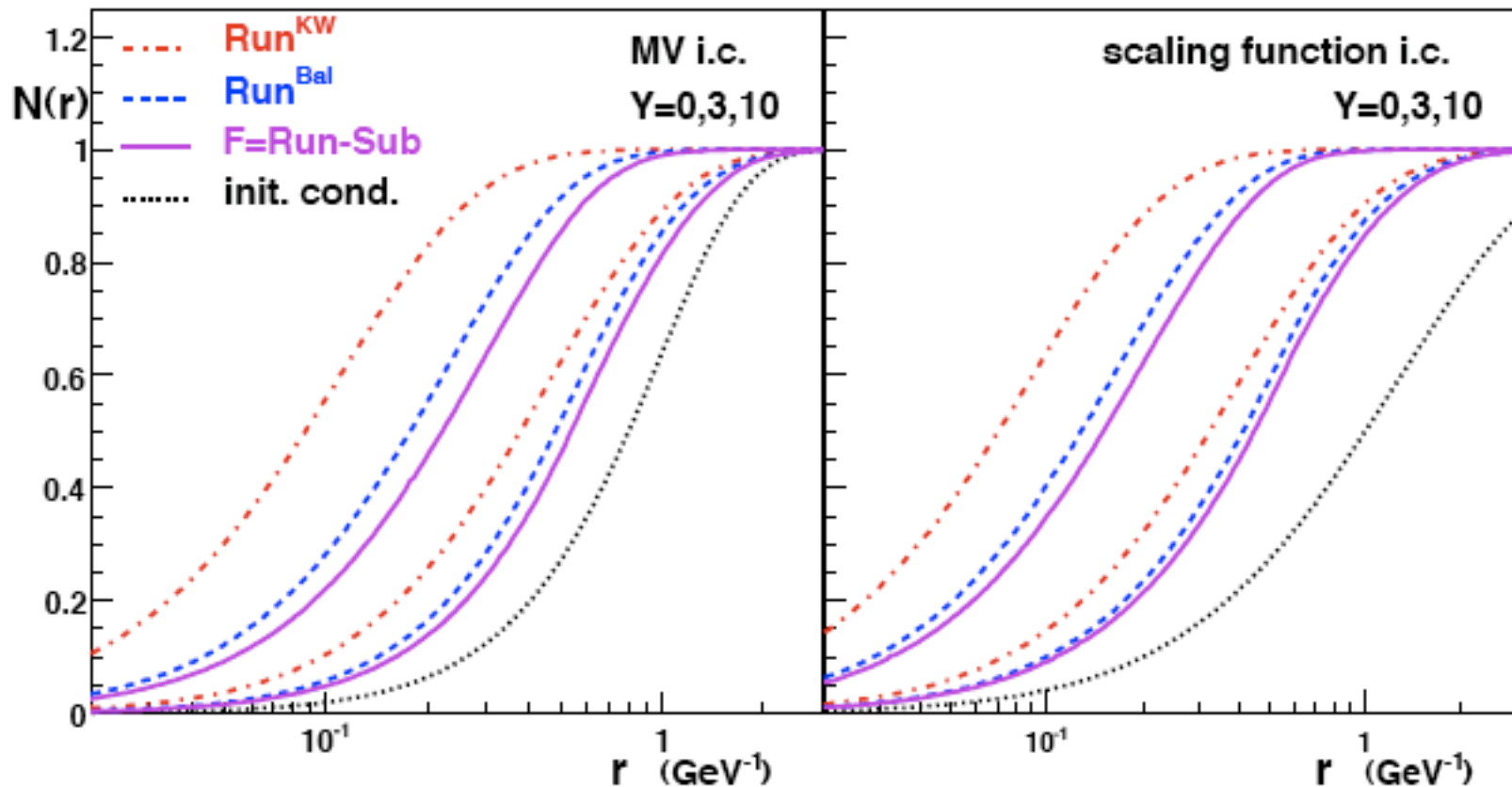
⇒ They result in two different kernels for the running coupling kernel:

$$\text{KW: } \tilde{K}_{KW}(\underline{r}, \underline{r}_1, \underline{r}_2) = \frac{N_c}{2\pi^2} \left[ \frac{\alpha_s(r_1^2)}{r_1^2} - 2 \frac{\alpha_s(r_1^2)\alpha_s(r_2^2)}{\alpha_s(R^2)} + \frac{\alpha_s(r_2^2)}{r_2^2} \right]$$

$$\text{BAL: } \tilde{K}_{Bal}(\underline{r}, \underline{r}_1, \underline{r}_2) = \frac{N_c \alpha_s(r^2)}{2\pi^2} \left[ \frac{r^2}{r_1^2 r_2^2} + \frac{1}{r_1^2} \left( \frac{\alpha_s(r_1^2)}{\alpha_s(r_2^2)} - 1 \right) + \frac{1}{r_2^2} \left( \frac{\alpha_s(r_2^2)}{\alpha_s(r_1^2)} - 1 \right) \right]$$

⇒ In both cases, running coupling comes in a “triumvirate”

⇒ Balitsky’s separation scheme minimizes the role of the subtraction term.





# Fixed vs Running

⇒ The **running of the coupling** reduces the speed of the evolution down to values compatible with experimental data (JLA PRL 99 262301 (07)):

$$\frac{\partial S}{\partial Y} = \mathcal{R}[S] - \mathcal{S}[S]$$

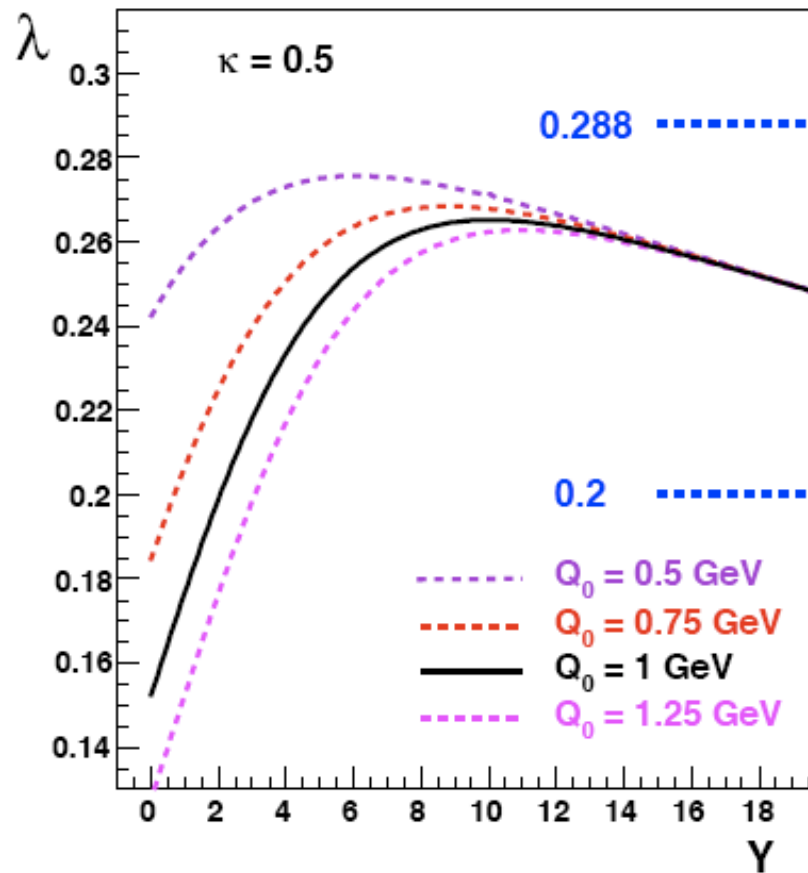
$$\lambda = \frac{d \ln Q_s^2(Y)}{dY}$$

LL evolution:

$$\lambda^{LL} \approx 4.8 \alpha_s$$

DIS data:

$$\lambda^{DIS} \approx 0.288$$



# Fixed vs Running

⇒ The **running of the coupling** reduces the speed of the evolution down to values compatible with experimental data (JLA PRL 99 262301 (07)):

$$\frac{\partial S}{\partial Y} = \mathcal{R}[S] - \mathcal{S}[S]$$

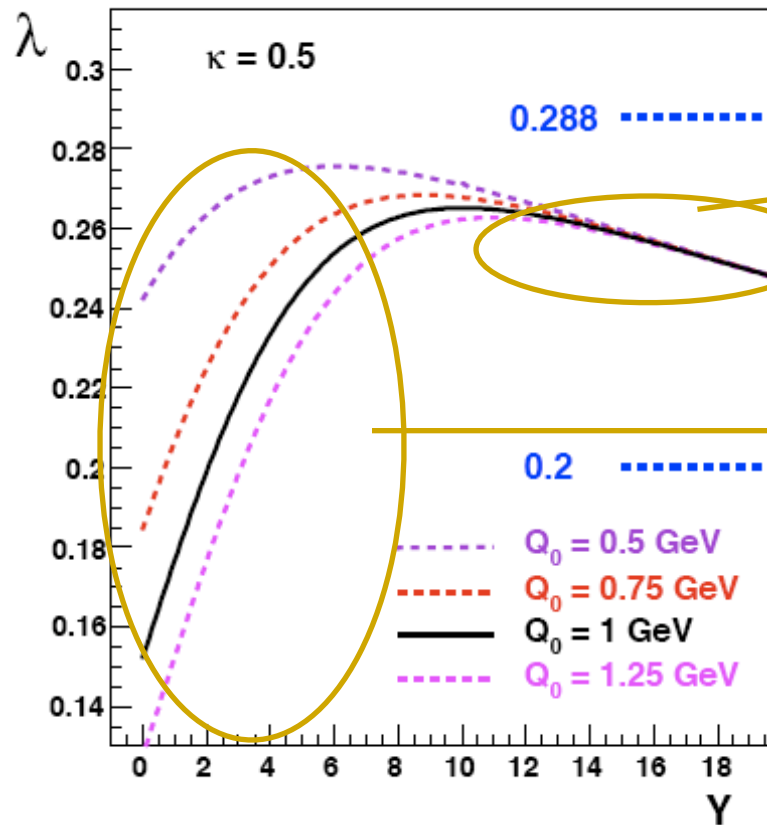
$$\lambda = \frac{d \ln Q_s^2(Y)}{dY}$$

LL evolution:

$$\lambda^{LL} \approx 4.8 \alpha_s$$

DIS data:

$$\lambda^{DIS} \approx 0.288$$



Geometric scaling

$$\lambda \sim \frac{1}{\sqrt{Y}}$$

Pre-asymptotic

⇒ The geometric scaling regime (independence on the initial conditions) is reached only at ultra-high energies

⇒ Fits to inclusive DIS structure function  $F_2(x, Q^2) = \frac{Q^2}{4\pi^2 \alpha_{em}} (\sigma_T + \sigma_L)$  for  $x \leq 10^{-2}$ . 3 active flavors.

$$\sigma_{T,L}(x, Q^2) = \sigma_0 \int_0^1 dz \int d^2\mathbf{r} \left| \Psi_{T,L}^{\gamma^* \rightarrow q\bar{q}}(z, Q, r) \right|^2 \mathcal{N}(x, r)$$

⇒ x-dependence: translational invariant running coupling BK using Balitsky's prescription

$$\frac{\partial \mathcal{N}(x, r)}{\partial \ln(x_0/x)} = \int d^2r_1 K^{Bal}(\mathbf{r}, \mathbf{r}_1, \mathbf{r}_2) [\mathcal{N}(x, r_1) + \mathcal{N}(x, r_2) - \mathcal{N}(x, r) - \mathcal{N}(x, r_1)\mathcal{N}(x, r_2)]$$

$$K^{Bal}(\mathbf{r}, \mathbf{r}_1, \mathbf{r}_2) = \frac{N_c \alpha_s(r^2)}{2\pi^2} \left[ \frac{r^2}{r_1^2 r_2^2} + \frac{1}{r_1^2} \left( \frac{\alpha_s(r_1^2)}{\alpha_s(r_2^2)} - 1 \right) + \frac{1}{r_2^2} \left( \frac{\alpha_s(r_2^2)}{\alpha_s(r_1^2)} - 1 \right) \right]$$

⇒ Regularization of the coupling: We freeze to a constant,  $\alpha_{fr}=0.7$  in the IR:

$$\alpha_s(r^2) = \frac{12\pi}{(11N_c - 2N_f) \ln\left(\frac{4C^2}{r^2 \Lambda_{QCD}}\right)} \quad \text{for } r < r_{fr}, \quad \text{with } \alpha_s(r_{fr}^2) \equiv \alpha_{fr} = 0.7$$

$$\alpha_s(r^2) = \alpha_{fr} = 0.7 \quad \text{for } r > r_{fr} \quad \Lambda_{QCD} = 0.241 \text{ GeV}$$

⇒ **Initial Conditions.** Inspired in the GBW and MV models:

$$\text{A) } \mathcal{N}^{GBW}(r, x_0 = 10^{-2}) = 1 - \exp \left[ - \left( \frac{r^2 Q_{s0}^2}{4} \right)^\gamma \right]$$

$$\text{B) } \mathcal{N}^{MV}(r, x_0 = 10^{-2}) = 1 - \exp \left[ - \left( \frac{r^2 Q_{s0}^2}{4} \right)^\gamma \ln \left( \frac{1}{r \Lambda_{QCD}} \right) \right]$$

Free parameters: proton saturation scale at  $x_0=10^{-2}$ ,  $Q_{s0}^2$ , and anomalous dimension,  $\gamma$

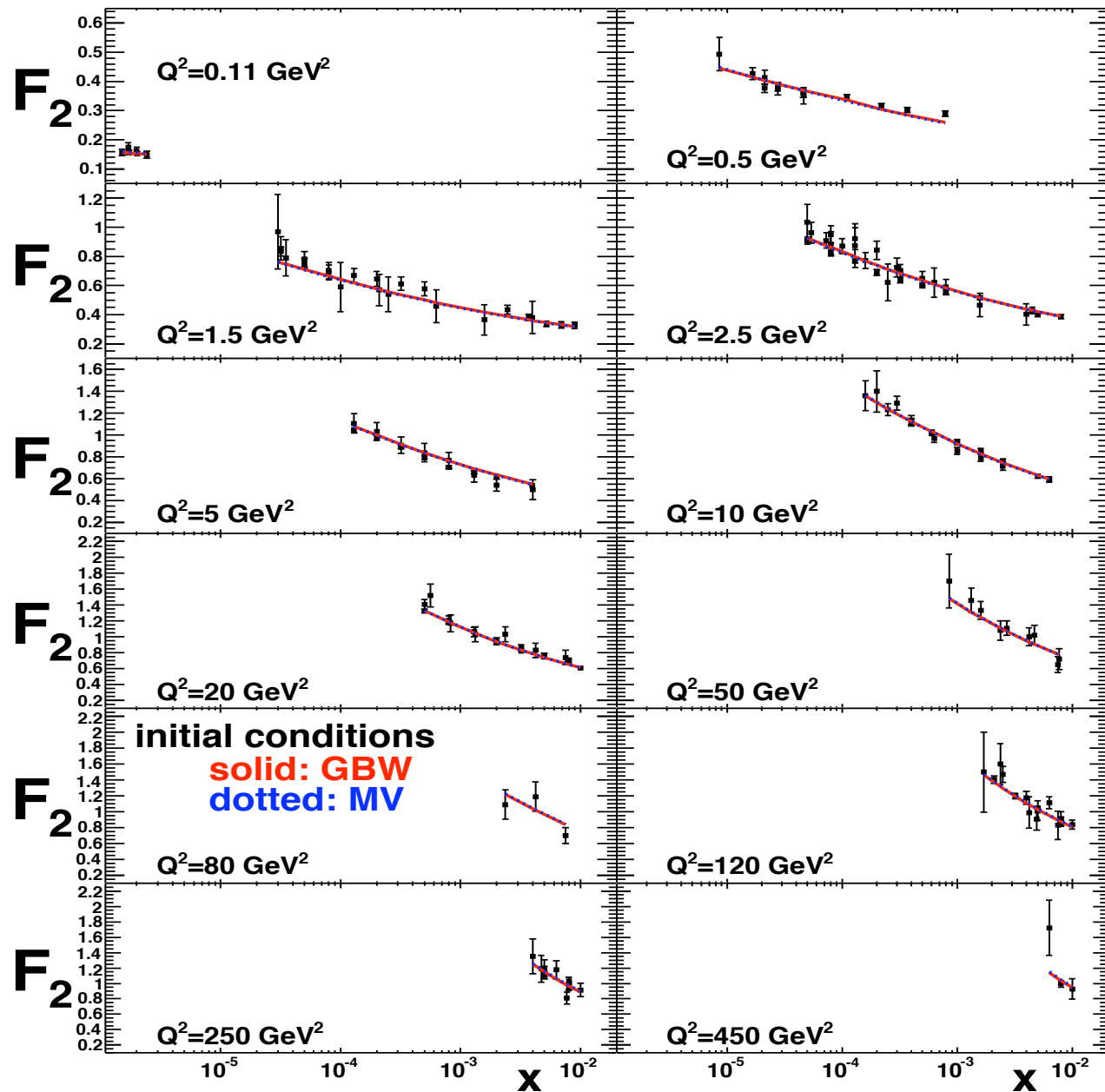
⇒ **Experimental data:** ZEUS, H1 (HERA), NMC (CERN-SPS) and E665 (Fermilab) coll.

$$\begin{array}{ll} 0.045 < Q^2 < 800 \text{ GeV}^2 & \mathbf{847 \text{ data points}} \\ x \leq 10^{-2} & \\ 0.045 < Q^2 < 50 \text{ GeV}^2 & \mathbf{703 \text{ data points}} \end{array}$$

**Fits are stable when large  $Q^2$  data are not included in the fit**

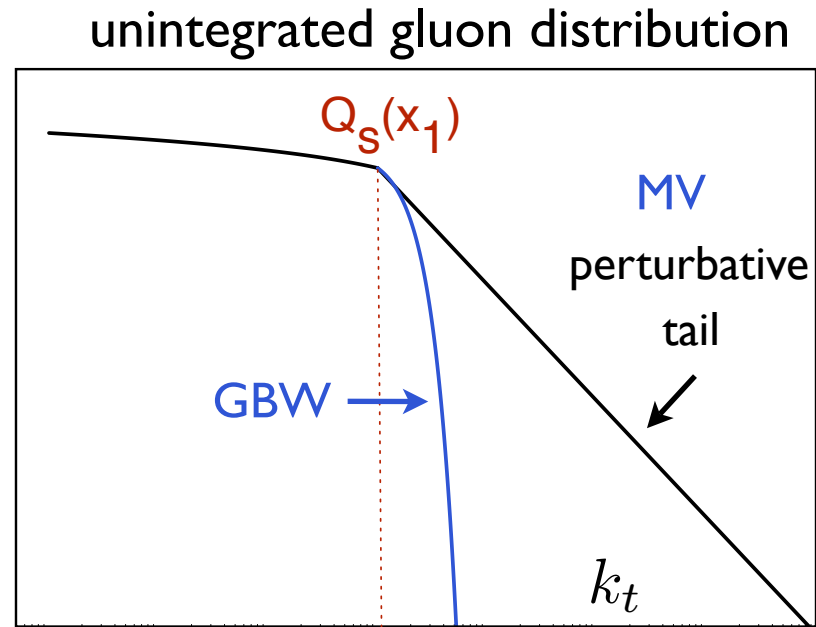
⇒ **3 (4) free parameters:** Normalization,  $\sigma_0$ , initial saturation scale,  $Q_{s0}^2$   
IR parameter,  $C^2$  (anomalous dimension of the i.c.  $\gamma$ )

Initial condition	$\sigma_0$ (mb)	$Q_{s0}^2$ (GeV <sup>2</sup> )	$C^2$	$\gamma$	$\chi^2/\text{d.o.f.}$
GBW	31.59	0.24	5.3	1 (fixed)	916.3/844=1.086
MV	32.77	0.15	6.5	1.13	906.0/843=1.075



## Lessons from the fits:

⇒ Fits to F2 do not constrain much the shape of the initial condition



⇒ In our set up, it is impossible to fit F2 data using linear BFKL evolution:

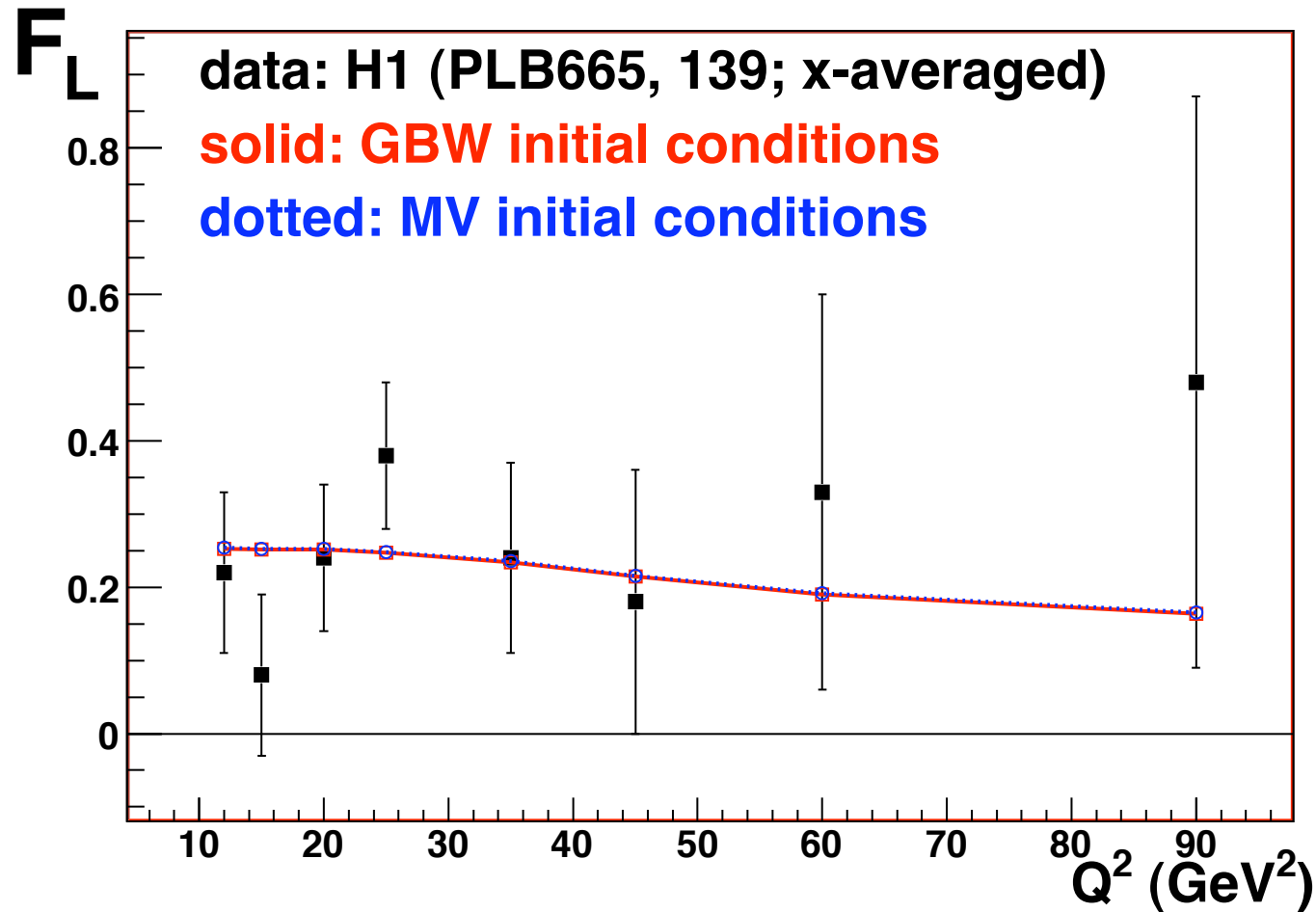
$$\frac{\partial \mathcal{N}(x, r)}{\partial \ln(x_0/x)} = \int d^2 r_1 K^{Bal}(\mathbf{r}, \mathbf{r}_1, \mathbf{r}_2) [\mathcal{N}(x, r_1) + \mathcal{N}(x, r_2) - \mathcal{N}(x, r) - \mathcal{N}(x, r_1)\mathcal{N}(x, r_2)]$$

⇒ Fits are stable after removing the higher  $Q^2$  data ( $> 50 \text{ GeV}^2$ )

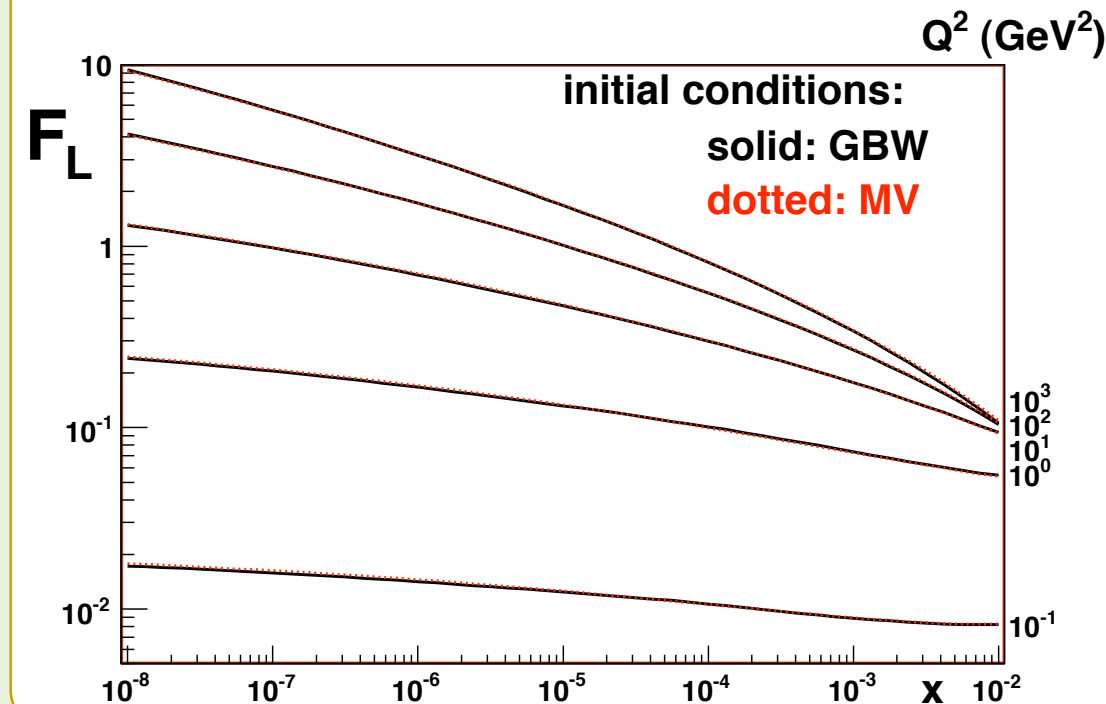
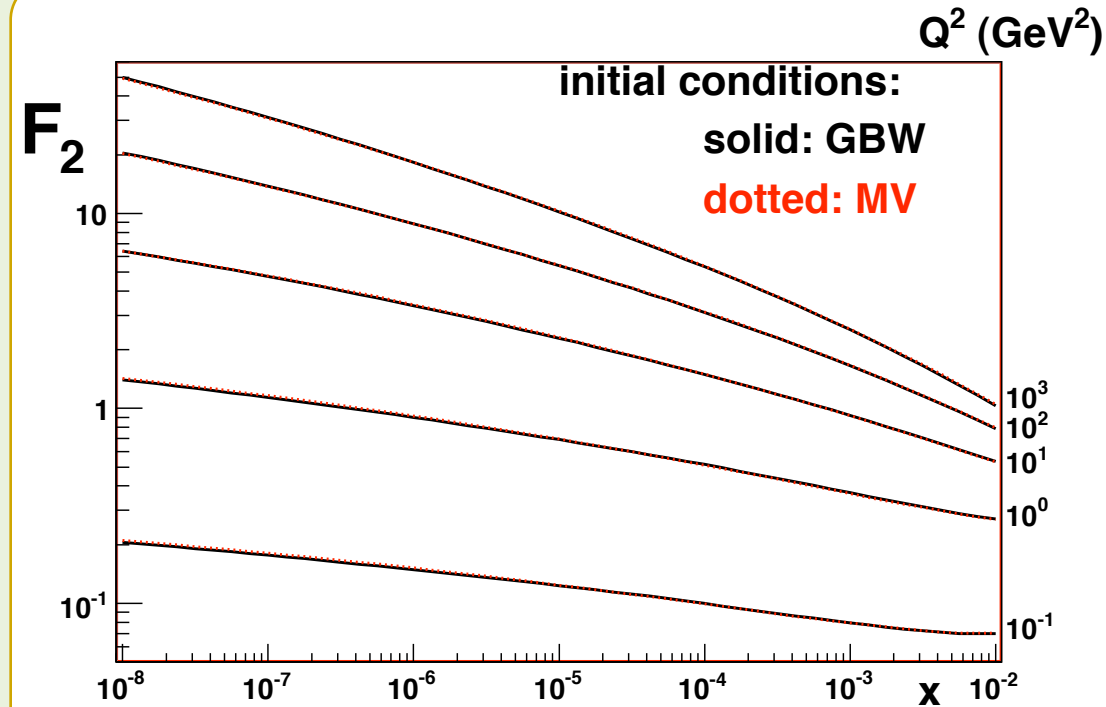
⇒ Fits are little sensitive to the prescription followed to regularize the coupling in the IR

⇒ Good description of the longitudinal structure function:

$$F_L(x, Q^2) = \frac{Q^2}{4\pi^2 \alpha_{em}} \sigma_L$$



## ⇒ Predictions for future colliders EIC, LHeC:

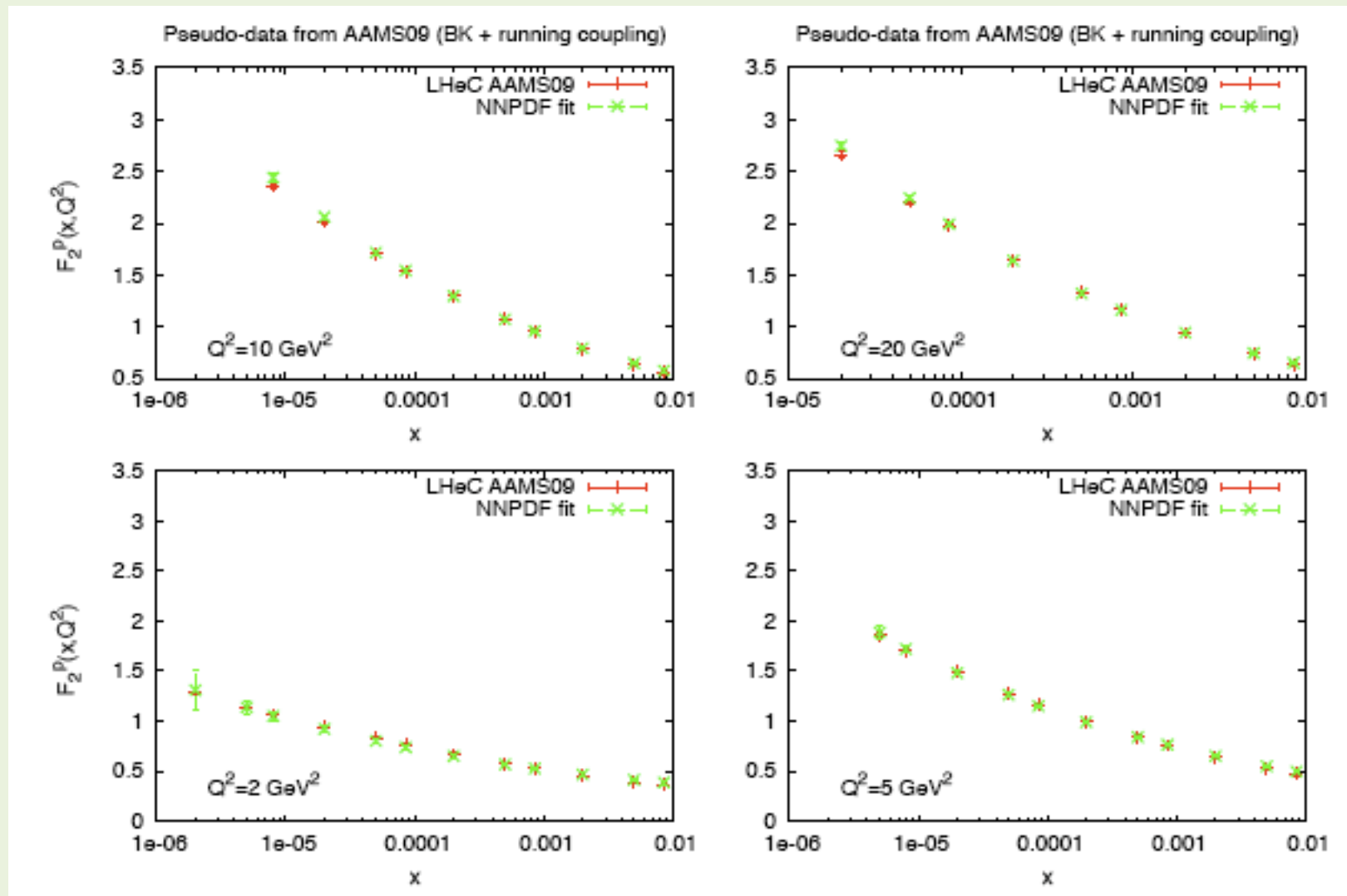


- Extrapolation to lower- $x$  completely driven by non-linear  $p$ QCD dynamics
- Almost insensitive to i.c. Good!!!
- Saturation effects are stronger for  $F_L$  than for  $F_2$
- $F_L$  is a very sensitive probe of the gluon d.f. Different calculations yield pretty different predictions in the low- $x$  low- $Q^2$  region



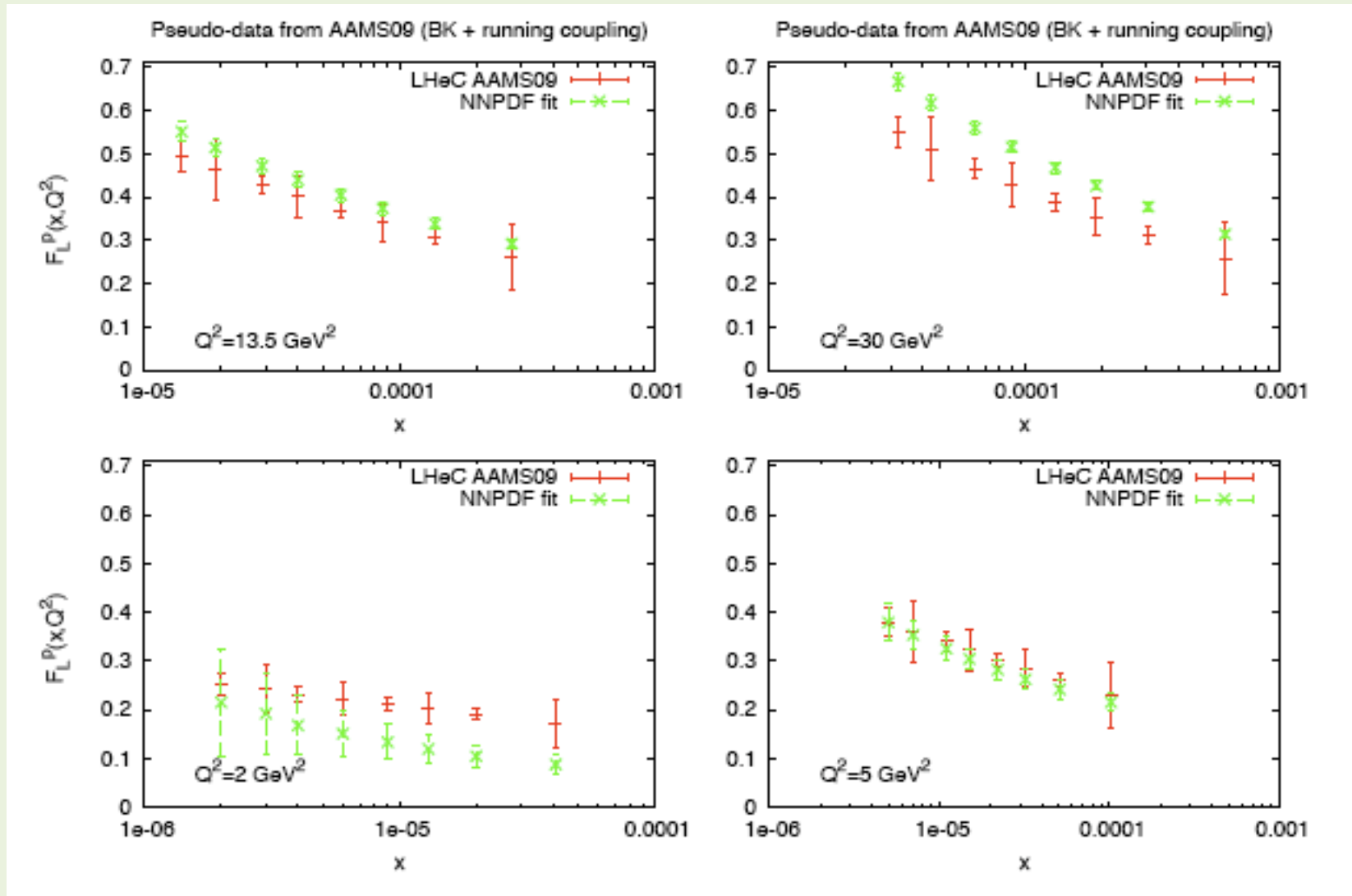
⇒ BK vs DGLAP at small-x (thanks to Juan Rojo):

DGLAP (NNPDF fit) can fit pseudodata for F2 at small-x generated by BK with running coupling:



## ⇒ BK vs DGLAP at small-x (thanks to Juan Rojo):

However, DGALP fails to reproduce pseudodata for FL at small-x:

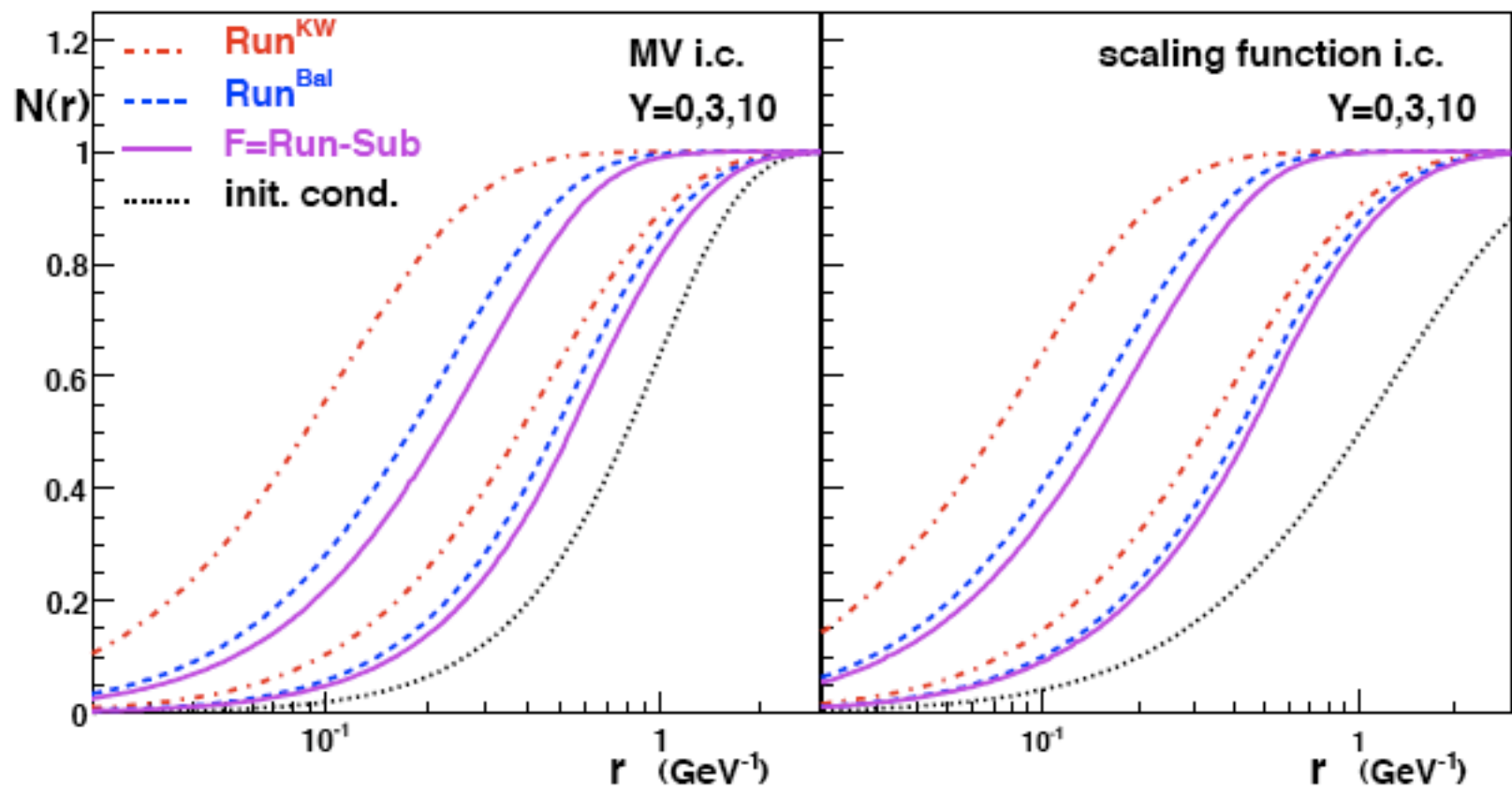


The divergence between linear DGLAP analyses and non-linear small-x dynamics is visible in FL already for  $x \sim 10^{-4}$

## SUMMARY

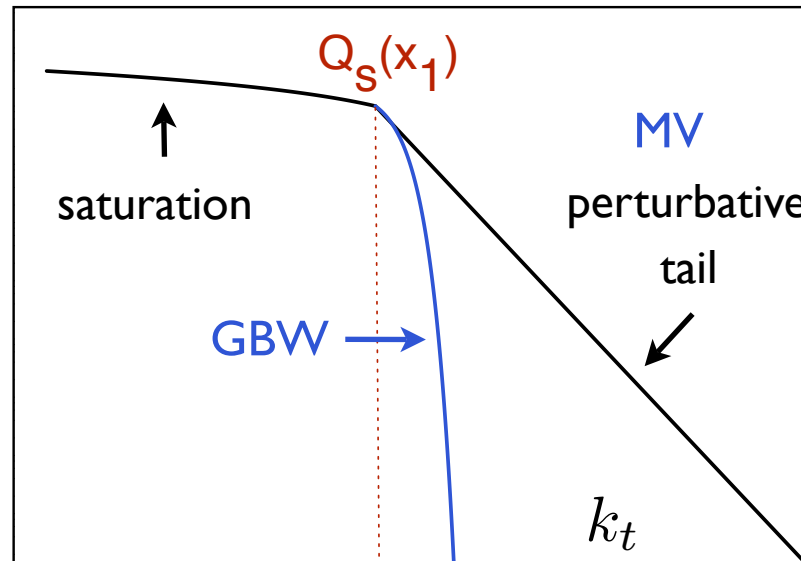
- Running coupling corrections to BK equation reconcile phenomenology and theory.
  - Successful fits to inclusive DIS data using BK with running coupling.
  - This is a first step in a bigger project for having non-linear pQCD controlled extrapolations to small- $x$  (LHeC, EIC, LHC, cosmic rays) for many different observables
  - Things to do next: include charm, impact parameter, nuclei...
- 
- Parametrizations of the proton-dipole amplitude available at <http://www-fp.usc.es/phenom/software.html>

**BACK UP SLIDES**



⇒ F2 is a too inclusive observable. Unable to discriminate between very different UV behaviour of the dipole amplitude. Need to compare to more exclusive observable (inclusive particle spectra in p-p collisions)

unintegrated gluon distribution: 
$$\varphi(x, k_t) = \int \frac{d^2 r}{2\pi r^2} \exp[i k_t \cdot r] \mathcal{N}(x, r)$$



⇒ Energy and rapidity dependence of hadron multiplicities in Au-Au collisions at RHIC:

- $k_t$ -factorization 'a la Kharzeev-Levin-Nardi'

$$\frac{dN_{AA}}{d\eta} \propto \frac{4\pi N_c}{N_c^2 - 1} \int^{p_m} \frac{d^2 p_t}{p_t^2} \int^p d^2 k_t \alpha_s(Q) \varphi_A \left( x_1; \frac{|p_t + k_t|}{2} \right) \varphi_A \left( x_2; \frac{|p_t - k_t|}{2} \right)$$

$\varphi(x, k) \Rightarrow$  Complete in  $\alpha_s$  Nf BK equation using MV i.c.  $\times (1-x)^4$

$$\frac{\partial S}{\partial Y} = \mathcal{R}[S] - \mathcal{S}[S]$$

• 2→1 kinematics

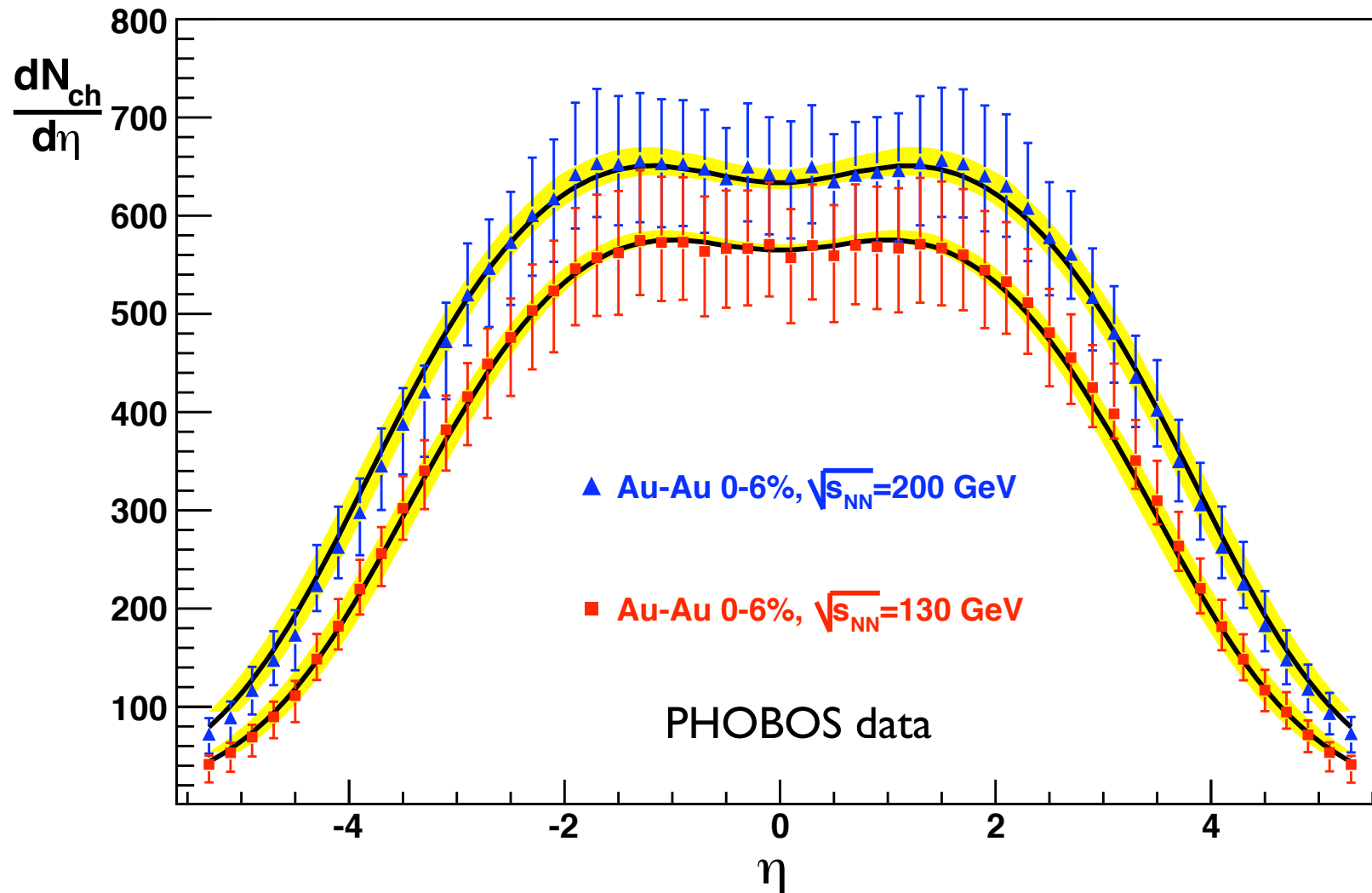
$$x_{1(2)} = \frac{p_t}{\sqrt{s}} e^{\pm y}$$

Local Hadron Parton Duality

⇒ 4 free parameters: Overall normalization, initial gold nucleus saturation scale (using MV initial condition), starting value of  $x$  for the evolution, average hadron mass

- Very good description of data at collision energies 130 and 200 GeV per nucleon:

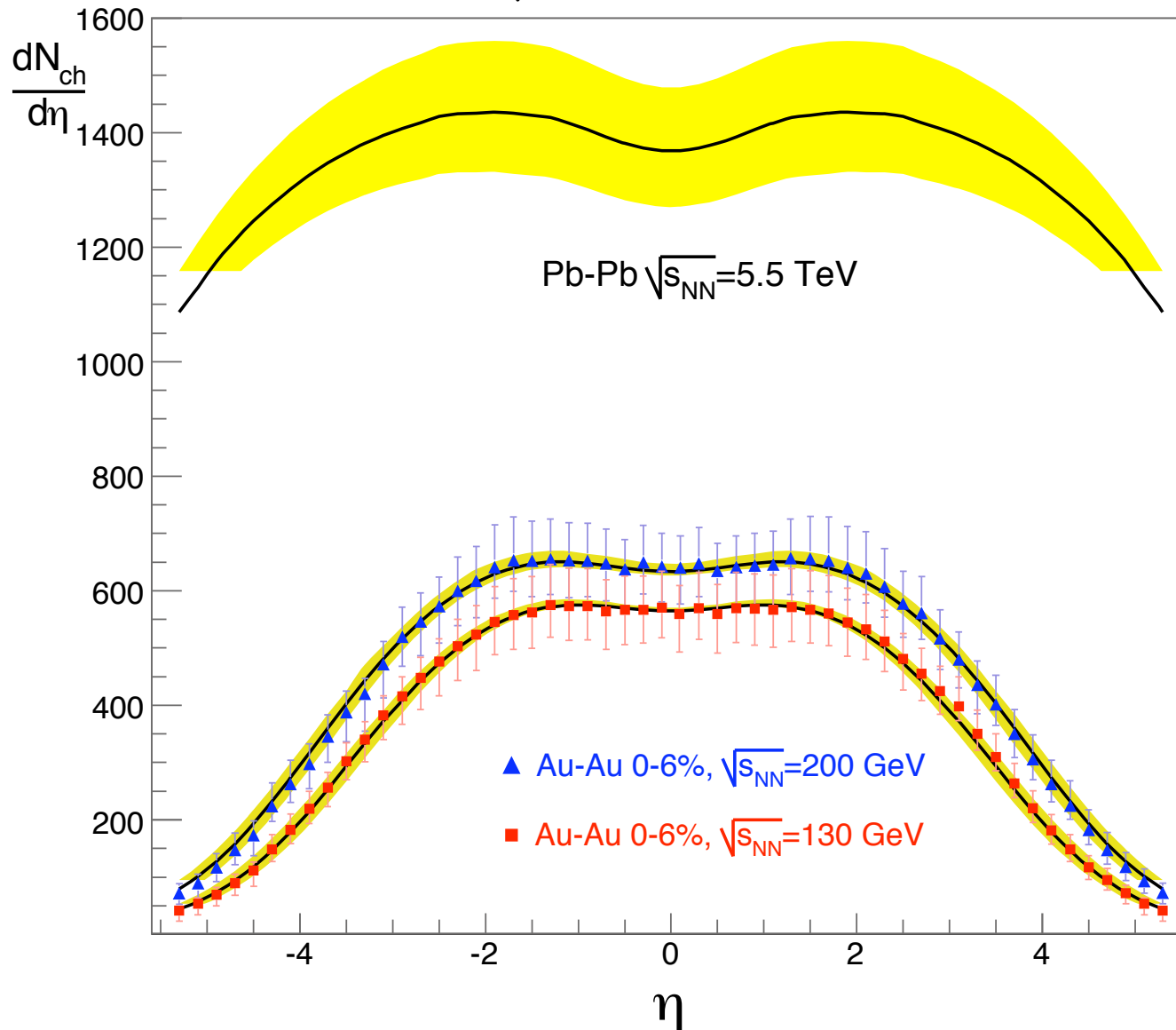
$$Q_0^2_{Au} \sim 0.75 \div 1.25 \text{ GeV}$$





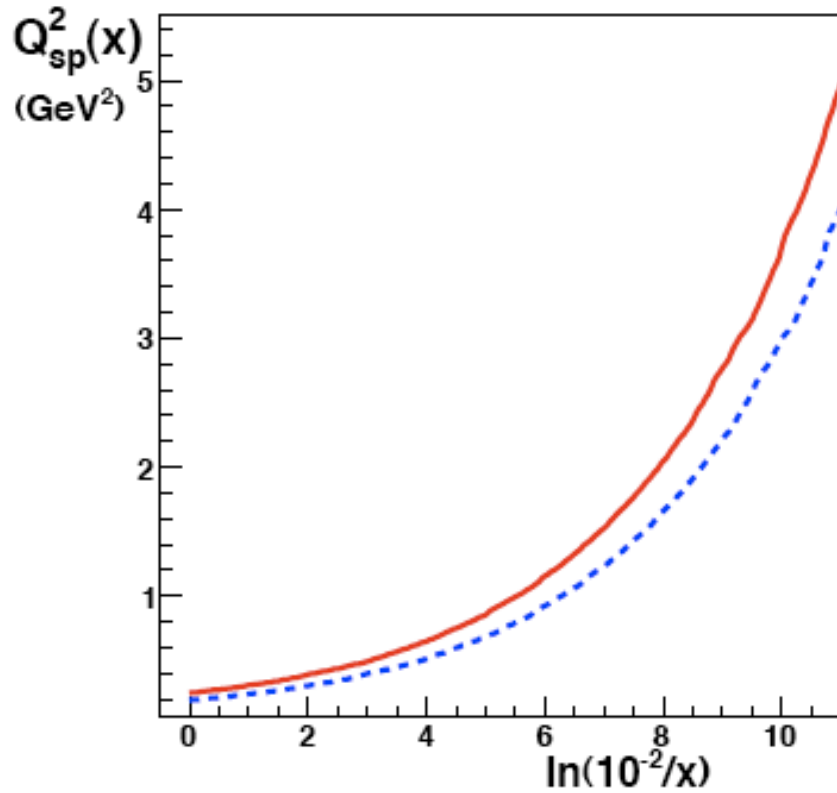
- Predictions for Pb-Pb collisions at the LHC are now completely driven by small-x evolution

$$\frac{dN_{ch}^{Pb-Pb}(\sqrt{s} = 5.5 \text{ TeV}, \eta = 0)}{d\eta} \approx 1290 \div 1480$$



**Saturation scale @ LHC**    kinematics:  $x \sim \frac{M}{\sqrt{s}} e^{-y}$     with  $M = 1 \text{ GeV}$

$$\mathcal{N}(r = 1/Q_s(x), x) = \kappa = 1 - e^{-0.25}$$



	<b>Pb</b>	<b>proton</b>
	$\sqrt{s} = 5.5 \text{ TeV}$	$\sqrt{s} = 14 \text{ TeV}$
$y$	$Q_s^2$ (GeV <sup>2</sup> )	$Q_s^2$ (GeV <sup>2</sup> )
0	2 ÷ 2.5	0.65 ÷ 0.85
2	3.2 ÷ 3.9	1.2 ÷ 1.5
4	5.2 ÷ 7	2.2 ÷ 2.7
6	9 ÷ 12	4 ÷ 5

⇒ Saturation effects may be sizable (detectable) in p-p collisions, specially at forward rapidities

- The dominant contribution to the evolution is given by the **running** term
- Balitsky's separation scheme minimizes the role of the subtraction term w.r.t. to KW's one

$$\frac{\partial S}{\partial Y} = \mathcal{R}[S] - \mathcal{S}[S]$$

